Formation and Chemical Reactivities of a New Type of Double-Butterfly $[\{Fe_2(\mu\text{-}CO)(CO)_6\}_2(\mu\text{-}SZS\text{-}\mu)]^{2-}$: Synthetic and Structural Studies on Novel Linear and Macrocyclic Butterfly Fe/E (E = S, Se) Cluster Complexes

Li-Cheng Song,* Hong-Tao Fan, Qing-Mei Hu, Zhi-Yong Yang, Yi Sun, and Feng-Hua Gong[a]

Abstract: A new type of double-butterfly $[\{Fe_2(\mu\text{-}CO)(CO)_6\}_2(\mu\text{-}SZS\text{-}\mu)]^{2-}$ (**3**), a dianion that has two μ-CO ligands, has been synthesized from dithiol HSZSH ($Z = (CH_2)_4$, $CH_2(CH_2OCH_2)_{1\text{-}3}CH_2$), $[Fe_3(CO)_{12}]$, and Et_3N in a molar ratio of 1:2:2 at room temperature. Interestingly, the in situ reactions of dianions **3** with various electrophiles affords a series of novel linear and macrocyclic butterfly Fe/E (E = S, Se) cluster complexes. For instance, while reactions of **3** with PhC(O)Cl and Ph_2PCl give linear clusters $[\{Fe_2(\mu\text{-}PhCO)(CO)_6\}_2(\mu\text{-}SZS\text{-}\mu)]$ (**4a**,**b**: $Z = CH_2(CH_2OCH_2)_{2,3}CH_2$) and $[\{Fe_2(\mu\text{-}Ph_2P)(CO)_6\}_2(\mu\text{-}SZS\text{-}\mu)]$ (**5a**,**b**: $Z = CH_2(CH_2OCH_2)_{2,3}CH_2$), reactions with CS_2 followed by treatment with monohalides RX or dihalides X−Y−X give both linear clusters $[\{Fe_2(\mu\text{-}RCS_2)(CO)_6\}_2(\mu\text{-}SZS\text{-}\mu)]$ (**6a**–**e**: $Z = CH_2(CH_2OCH_2)_{1,2}CH_2$; R = Me, $PhCH_2$, $FeCp(CO)_2$) and macrocyclic clusters $[\{Fe_2(CO)_6\}_2(\mu\text{-}SZS\text{-}\mu)\text{-}(\mu\text{-}CS_2YCS_2\text{-}\mu)]$ (**7a**–**e**: $Z = (CH_2)_4$, $CH_2(CH_2OCH_2)_{1\text{-}3}CH_2$; $Y = (CH_2)_{2\text{-}4}$, 1,3,5-$Me(CH_2)_2C_6H_3$, 1,4-$(CH_2)_2C_6H_4$). In addition, reactions of dianions **3** with $[Fe_2(\mu\text{-}S_2)(CO)_6]$ followed by treatment with RX or X−Y−X give linear clusters $[\{[Fe_2(CO)_6]_2(\mu\text{-}RS)(\mu_4\text{-}S)\}_2(\mu\text{-}SZS\text{-}\mu)]$ (**8a**–**c**: $Z = CH_2(CH_2OCH_2)_{1,2}CH_2$; R = Me, $PhCH_2$) and macrocyclic clusters $[\{[Fe_2(CO)_6]_2(\mu_4\text{-}S)\}_2(\mu\text{-}SYS\text{-}\mu)(\mu\text{-}SZS\text{-}\mu)]$ (**9a**,**b**: $Z = CH_2(CH_2OCH_2)_{2,3}CH_2$; $Y = (CH_2)_4$), and reactions with $SeCl_2$ afford macrocycles $[\{Fe_2(CO)_6\}_2\text{-}(\mu_4\text{-}Se)(\mu\text{-}SZS\text{-}\mu)]$ (**10d**: $Z = CH_2\text{-}(CH_2OCH_2)_3CH_2$) and $[\{[Fe_2(CO)_6]_2\text{-}(\mu_4\text{-}Se)\}_2(\mu\text{-}SZS\text{-}\mu)_2]$ (**11a**–**d**: $Z = (CH_2)_4$, $CH_2(CH_2OCH_2)_{1\text{-}3}CH_2$). Production pathways have been suggested; these involve initial nucleophilic attacks by the Fe-centered dianions **3** at the corresponding electrophiles. All the products are new and have been characterized by combustion analysis and spectroscopy, and by X-ray diffraction techniques for **6c**, **7d**, **9b**, **10d**, and **11c** in particular. X-ray diffraction analyses revealed that the double-butterfly cluster core Fe_4S_2Se in **10d** is severely distorted in comparison to that in **11c**. In view of the Z chains in **10a**–**c** being shorter than the chain in **10d**, the double cluster core Fe_4S_2Se in **10a**–**c** would be expected to be even more severely distorted, a possible reason for why **10a**–**c** could not be formed.

Keywords: cluster compounds · iron · macrocycles · structure elucidation

Introduction

During the last two decades there has been considerable interest in Fe/E (E = S, Se) cluster complexes, largely due to the structural novelty, versatility and reactivity of such materials,[1] as well as their potential applications, for example, their use as models for the active sites on non-heme iron protein ferredoxins[2] and the Fe-only hydrogenases.[3] Among the Fe/E cluster complexes the butterfly monoanions containing one μ-CO ligand, $[Fe_2(\mu\text{-}RE)(\mu\text{-}CO)(CO)_6]^-$ (**1**) (E = S, Se)[4–15] and $[\{Fe_2(CO)_6\}_2(\mu\text{-}RS)(\mu\text{-}CO)(\mu_4\text{-}S)]^-$ (**2**),[16] have been shown to be very useful versatile synthons in the synthesis of a wide variety of linear butterfly Fe/E cluster complexes.[4–16] To further develop the chemistry of Fe/E clusters, we investigated whether the butterfly Fe/S cluster

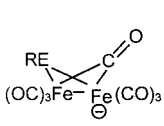

1

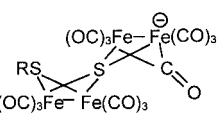

2

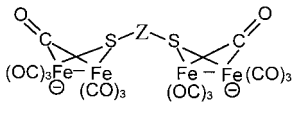

3

[a] Prof. L.-C. Song, Dr. H.-T. Fan, Prof. Q.-M. Hu, Dr. Z.-Y. Yang, Dr. Y. Sun, Dr. F.-H. Gong
Department of Chemistry
State Key Laboratory of Elemento-Organic Chemistry
Nankai University, Tianjin 300071 (China)
Fax: (+86) 22-23504853
E-mail: lcsong@public.tpt.tj.cn

0947-6539/03/0901-0170 $ 20.00+.50/0

dianions containing two μ-CO ligands of the type $[\{Fe_2(\mu\text{-}CO)(CO)_6\}_2(\mu\text{-}SZS\text{-}\mu)]^{2-}$ (**3**) could be formed, and if it could serve as another type of important synthon to give not only the linear butterfly clusters, but also the butterfly clusters with unique cyclic structures. In a recent communication,[17] we preliminarily reported the formation of dianions **3** with $Z = CH_2(CH_2OCH_2)_{2,3}CH_2$ and their in situ reactions leading to four macrocyclic butterfly clusters.

In this article we will systematically describe the formation of the two μ-CO-containing double-butterfly cluster dianions **3** with $Z = (CH_2)_4$ and $CH_2(CH_2OCH_2)_{1-3}CH_2$, and their in situ reactions with several types of electrophiles, such as PhC(O)Cl, Ph_2PCl, CS_2/monohalides, CS_2/dihalides, $[Fe_2(\mu\text{-}S_2)(CO)_6]$/monohalides, $[Fe_2(\mu\text{-}S_2)(CO)_6]$/dihalides, and $SeCl_2$, which afford a series of new types of novel linear and macrocyclic butterfly Fe/E cluster complexes. In addition, we describe the structural characterization of all the synthesized compounds, and the possible reaction pathways for production of these novel linear and macrocyclic cluster complexes.

Results and Discussion

Formation of dianions $[\{Fe_2(\mu\text{-}CO)(CO)_6\}_2(\mu\text{-}SZS\text{-}\mu)]^{2-}$ (3) from $[Fe_3(CO)_{12}]$, HSZSH and Et_3N. Reactions of 3 with PhC(O)Cl and Ph_2PCl leading to linear clusters $[\{Fe_2(\mu\text{-}PhCO)(CO)_6\}_2(\mu\text{-}SZS\text{-}\mu)]$(4a,b) and $[\{Fe_2(\mu\text{-}Ph_2P)(CO)_6\}_2(\mu\text{-}SZS\text{-}\mu)]$ (5a,b): We found that when a solution of dithiol HSZSH ($Z = (CH_2)_4$, $CH_2(CH_2OCH_2)_{1-3}CH_2$), $Fe_3(CO)_{12}$ and Et_3N in a molar ratio of 1:2:2 in THF was stirred at room temperature for approximately 0.5 h, the original green color of the solution changed to deep red. This indicated the formation of the $[Et_3NH]^+$ salts of a novel type of dianion **3**. The IR spectra of these deep red solutions showed an absorption band at approximately $\nu = 1744\ cm^{-1}$, characteristic of their μ-CO ligands. This is very similar to the IR spectrum of the solution containing the $[Et_3NH]^+$ salt of monoanion **1** (R = Et) in THF and exhibits a μ-CO absorption band at $\nu = 1743\ cm^{-1}$.[4] However, the intensities of the μ-CO bands displayed by these deep red solutions were markedly decreased when these solutions were exposed to air or refluxed under N_2. For example, when the solution of **3** with $Z = CH_2(CH_2OCH_2)_3CH_2$ was exposed to air or refluxed under N_2 for 15 min, the original intensity of its μ-CO band at 1742 cm^{-1} decreased by 60 and 70%, respectively. This means that dianions **3** are very air-sensitive and thermally unstable; therefore, we carried out their reactions in situ and at room temperature.

We further found that the in situ reactions of the $[Et_3NH]^+$ salts of dianions **3** ($Z = CH_2(CH_2OCH_2)_{2,3}CH_2$) with an excess of benzoyl chloride or one equivalent of diphenylchlorophosphine (initially through attack of two molecules of PhC(O)Cl or Ph_2PCl, respectively, at the two iron atoms of dianions **3**, followed by displacement of two μ-CO ligands in each of the intermediates **h** and **k**) gave rise to the corresponding linear double-butterfly cluster complexes $[\{Fe_2(\mu\text{-}PhCO)(CO)_6\}_2(\mu\text{-}SZS\text{-}\mu)]$ (**4a**,**b**) and $[\{Fe_2(\mu\text{-}Ph_2P)(CO)_6\}_2(\mu\text{-}SZS\text{-}\mu)]$ (**5a**,**b**) as shown in Scheme 1.

Clusters **4a**,**b** and **5a**,**b** are the first examples of the two μ-Ph_2P-containing double-butterfly Fe/S cluster complexes, although the corresponding single-butterfly Fe/S clusters with one such ligand, namely $[Fe_2(\mu\text{-}PhCO)(\mu\text{-}EtS)(CO)_6]$ and $[Fe_2(\mu\text{-}Ph_2P)(\mu\text{-}EtS)(CO)_6]$, were prepared in 1985.[4] In addition, the proposed pathways for the formation of **4a**,**b** and **5a**,**b** shown in Scheme 1 are primarily based on the well-known chemistry of the single-butterfly monoanions containing one μ-CO ligand $[Fe_2(\mu\text{-}RE)(\mu\text{-}CO)(CO)_6]^-$ (**1**) (E = S, Se).[4–15] This general sequence, in which dianions **3** act as iron-centered nucleophiles, has also served to explain the chemistry observed for dianions of type **3** as described below. Complexes **4a**,**b** and **5a**,**b** have been characterized by elemental analysis and spectroscopy. The IR spectra of **4a**,**b** and **5a**,**b** displayed three absorption bands in the range $\nu = 2074 - 1982\ cm^{-1}$ for their terminal carbonyls and one absorption band at approximately $\nu = 1110\ cm^{-1}$ for their bridged ether chain functionalities; in addition the spectra of **4a**,**b** showed one absorption band at $\nu = 1469\ cm^{-1}$ for their bridging benzoyl carbonyls.[4] The ^{13}C NMR spectra of **4a**,**b** exhibited a singlet at $\delta = 289$ ppm for their bridging acyl carbon atoms and the ^{31}P NMR spectra of **5a**,**b** showed a singlet at $\delta = 142$ ppm for their bridging P atoms; these data are consistent with those single-butterfly cluster complexes that contain the same cluster cores as **4a**,**b** and **5a**,**b**, respectively.[4, 18]

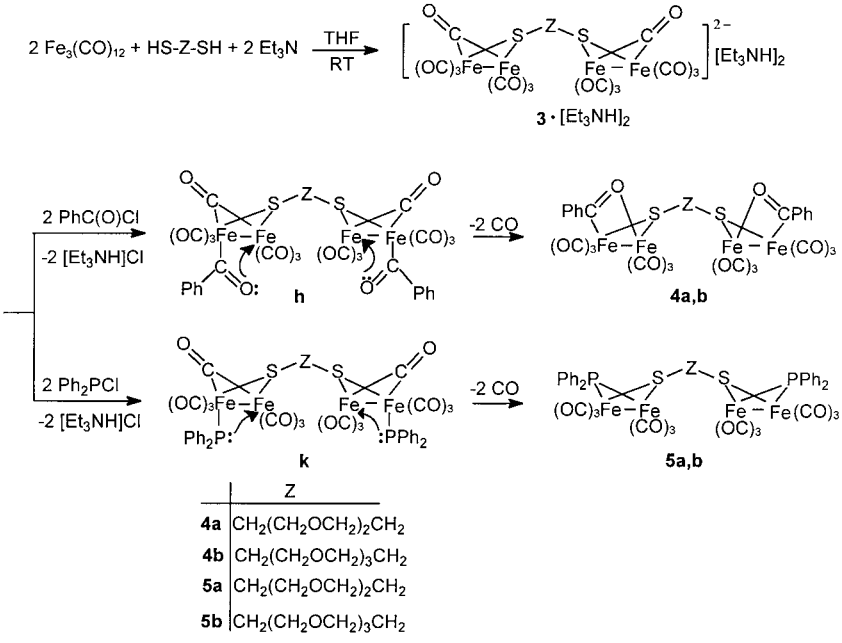

Scheme 1.

  0947-6539/03/0901-0171 $ 20.00+.50/0

In principle, clusters **4a**,**b** and **5a**,**b** may have three conformers (Scheme 2) in terms of the type of bonds (axial or equatorial) by which group Z is attached to the bridged S atoms in butterfly cluster cores.[19] However, since the

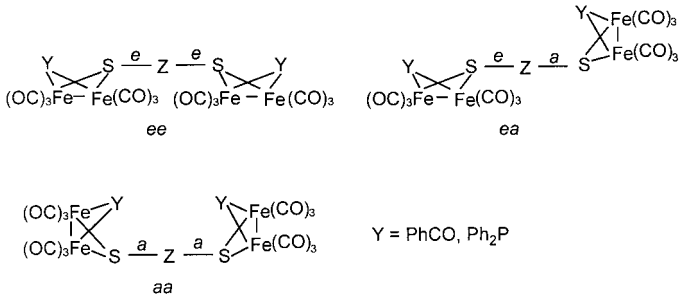

Scheme 2.

^{1}H NMR spectra of the two SCH_2 moieties of each Z group in **4a**,**b** and **5a**,**b** showed only one broad singlet at approximately $\delta = 2.7$ ppm, the Z group is most likely attached to the two S atoms by two equatorial bonds (note that if the Z group is attached to the two S atoms by two axial bonds, the singlet would be located at higher field with a chemical shift less than $\delta = 2$ ppm).[20] The fact that **4a**,**b** and **5a**,**b** exist as only one conformer is also consistent with the ^{13}C NMR spectra of the bridged acyl carbon atoms in **4a**,**b** and the ^{13}P NMR spectra of the bridged P atoms in **5a**,**b** as mentioned above. Although the equatorial–equatorial (ee) conformers of **4a**,**b** and **5a**,**b** have not been directly confirmed by their X-ray diffraction analyses due to lack of suitable crystals (**4a**,**b** and **5a**,**b** are either oils or solids with low melting points), they have been indirectly confirmed by X-ray diffraction analyses of the linear and macrocyclic clusters **6c**, **7d**, **9b**, **10d**, and **11c** containing the same type of Z groups (vide infra).

Reactions of 3 with CS_2/organic halides leading to linear clusters [{Fe_2(μ-RCS_2)$(CO)_6$}$_2$(μ-SZS-μ)] (6a–e) and macrocyclic clusters [{$Fe_2(CO)_6$}$_2$(μ-CS_2Y-CS_2-μ)(μ-SZS-μ)] (7a–e): We also found that when an excess of CS_2 was added to the solutions containing dianions **3** (Z = $CH_2(CH_2OCH_2)_{1-3}CH_2$), followed by treatment of the $[Et_3NH]^+$ salts of another type of dianion [{Fe_2(μ-S=C–S^-)$_2(CO)_6$}$_2$(μ-SZS-μ)] (**m**) with an equivalent or an excess of organic halides RX and X–Y–X, a series of linear and macrocyclic clusters [{Fe_2(μ-RCS_2)$(CO)_6$}$_2$(μ-SZS-μ)] (**6a–e**) and [{$Fe_2(CO)_6$}$_2$(μ-CS_2-Y-CS_2-μ)(μ-SZS-μ)] (**7a–e**) were produced (Scheme 3).

It is noteworthy that the formation of dianions **m** from dianions **3** and CS_2 is not unusual, because the reaction of monoanions **1** with CS_2 is known to give the single μ-CS_2-containing analogues of **m**, that is, monoanions [$Fe_2(CO)_6$(μ-RS)(μ-S=CS^-)].[21] In addition, while the yields of linear clusters **6a–e** are as high as 52–65%, those of macrocyclic clusters **7a–e** are only 11–16%. These low yields of **7a–e** are probably due to the complicated competitive reaction between the intramolecular ring-closure of intermediate $\mathbf{m_1}\cdot[Et_3NH]$ (to give macrocycles **7a–e**) and the intermolecular condensation of $\mathbf{m_1}\cdot[Et_3NH]$ (to give linear oligomers $\mathbf{m_2}\cdot[Et_3NH]$) (Scheme 4).

Both linear and cyclic clusters **6a–e** and **7a–e** are new and have been characterized by combustion analysis and spectroscopy. The IR spectra of these compounds showed several absorption bands in the range $\nu = 2074–1962$ cm^{-1} for their terminal carbonyls ligands and one absorption band in the region $\nu = 1019–1002$ cm^{-1} for their C=S functional groups coordinated to iron atoms. It is due to such a coordination mode that the absorption band of the thiocarbonyl C=S groups in **6a–e** and **7a–e** lies at a much lower frequency than that of C=S in free CS_2 (1533 cm^{-1}) and falls within the range 1120–860 cm^{-1} displayed by the coordinated C=S in some other transition metal complexes.[22] Similar to **4a**,**b** and **5a**,**b**, the Z group in each of **6a–e** and **7a–e** is most likely attached to the two bridging S atoms by two equatorial bonds, since the ^{1}H NMR spectra of the two SCH_2 of each Z group in **6a–e** and **7a–e** showed only one set of signals at $\delta =$ 2.5–3.1 ppm.[20] Fortunately, this assignment has been confirmed by X-ray diffraction analyses for **6c** and **7d** (vide infra).

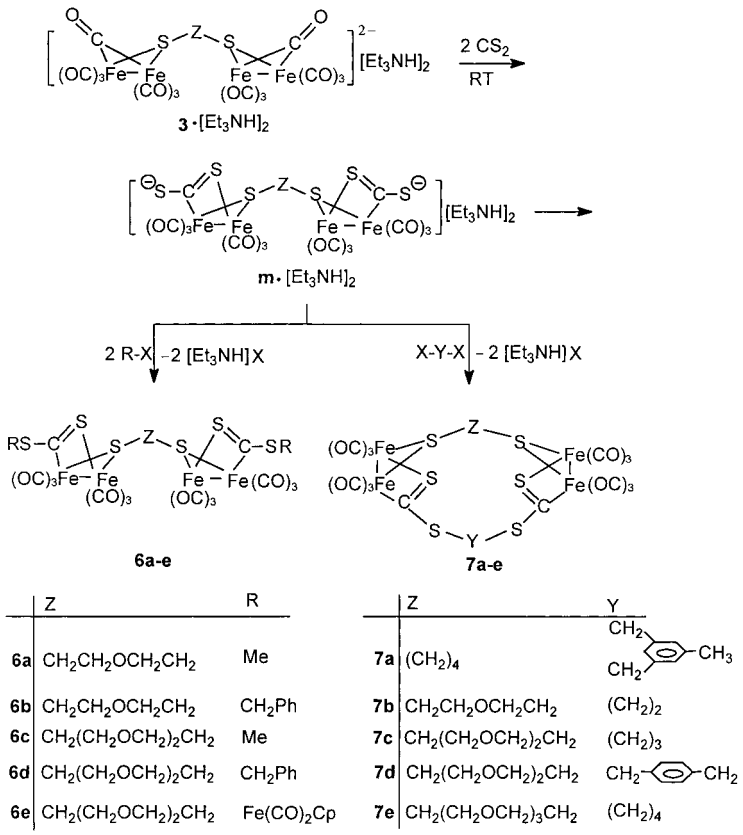

	Z	R
6a	$CH_2CH_2OCH_2CH_2$	Me
6b	$CH_2CH_2OCH_2CH_2$	CH_2Ph
6c	$CH_2(CH_2OCH_2)_2CH_2$	Me
6d	$CH_2(CH_2OCH_2)_2CH_2$	CH_2Ph
6e	$CH_2(CH_2OCH_2)_2CH_2$	$Fe(CO)_2Cp$

	Z	Y
7a	$(CH_2)_4$	
7b	$CH_2CH_2OCH_2CH_2$	$(CH_2)_2$
7c	$CH_2(CH_2OCH_2)_2CH_2$	$(CH_2)_3$
7d	$CH_2(CH_2OCH_2)_2CH_2$	
7e	$CH_2(CH_2OCH_2)_3CH_2$	$(CH_2)_4$

Scheme 3.

0947-6539/03/0901-0172 $ 20.00+.50/0 *Chem. Eur. J.* **2003**, *9*, No. 1

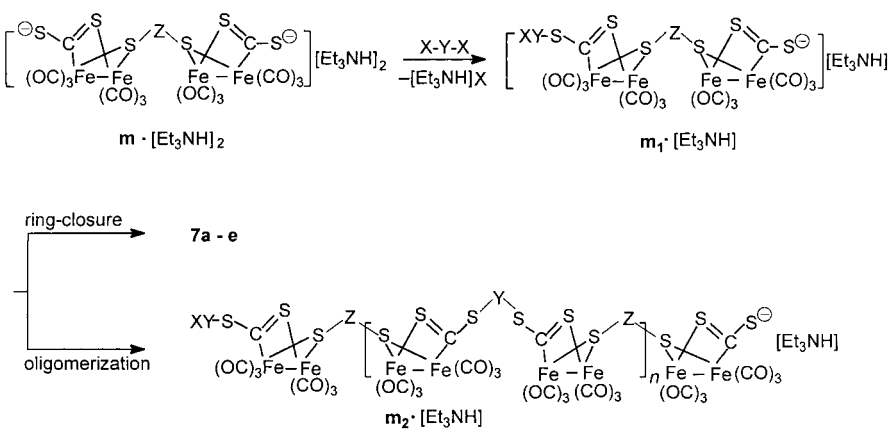

Scheme 4.

Crystal structures of 6c and 7d: To unambiguously confirm the structures of linear and cyclic products **6a–e** and **7a–e**, single-crystal X-ray diffraction analyses for **6c** and **7d** were carried out. Table 1 lists their selected bond lengths and angles, whereas Figures 1 and 2, respectively, display their molecular structures. Figure 1 shows that **6c** is a centrosymmetrical molecule and it consists of two single-butterfly cluster cores Fe(1)Fe(2)S(1)S(2)C(7) and Fe(1A)Fe(2A)-S(1A)S(2A)C(7A), which are indeed connected by the ether chain C(11)C(12)O(7)C(13)-C(13A)O(7A)C(12A)C(11A) with two equatorial bonds C(11)–S(1) and C(11A)–S(1A). All of the twelve carbonyls attached to iron atoms are terminal and the methyl groups are bonded to S(3) and S(3A) in an *endo* mode (namely C(8)–S(3) and C(8A)–S(3A) lie toward the inside of their attached two-butterfly subcluster cores, respectively). The thiocarbonyl C(7)=S(2) and C(7A)=S(2A) groups in double-butterfly cluster **6c**, similar to that of single-butterfly cluster $[Fe_2(\mu\text{-PhSe})(\mu\text{-PhCH}_2\text{SC=S})(CO)_6]$,[9] are coordinated to Fe(1) and Fe(1A), respectively, by σ bonds (Fe(1)–C(7) = Fe(1A)–C(7A) = 1.989(8) Å) with carbene character[22] and to Fe(2) and Fe(2A), respectively, through the donation of an unshared electron pair from S(2) or S(2A) (Fe(2)–S(2) = Fe(2)–S(2A) = 2.270(4) Å). The bond lengths of the thiocarbonyl C(7)=S(2) and C(7A)=S(2A) extend to 1.667(7) Å from 1.554 Å in free CS_2, and are very close to that found in $[Fe_2(\mu\text{-PhSe})(\mu\text{-PhCH}_2\text{SC=S})(CO)_6]$ (1.63(1) Å).[9]

Table 1. Selected bond lengths [Å] and angles [°] for **6c** and **7d**.

Complex **6c**			
Fe(1)–C(7)	1.989(8)	Fe(2)–S(2)	2.270(4)
Fe(1)–S(1)	2.248(3)	Fe(1)–C(11)	1.831(10)
Fe(1)–Fe(2)	2.616(3)	S(2)–C(7)	1.667(7)
Fe(2)–S(1)	2.235(3)	S(3)–C(8)	1.882(12)
C(7)-Fe(1)-S(1)	82.9(2)	S(1)-Fe(1)-Fe(2)	54.05(9)
C(7)-Fe(1)-Fe(2)	76.5(2)	S(2)-Fe(2)-Fe(1)	77.01(11)
S(1)-Fe(2)-S(2)	83.68(12)	Fe(2)-S(1)-Fe(1)	71.41(10)
S(1)-Fe(2)-Fe(1)	54.54(9)	S(2)-C(7)-Fe(1)	113.0(4)
Complex **7d**			
Fe(1)–C(13)	1.999(13)	Fe(3)–S(6)	2.252(4)
Fe(1)–S(2)	2.248(4)	Fe(3)–Fe(4)	2.615(3)
Fe(2)–S(2)	2.243(3)	Fe(4)–S(5)	2.297(3)
S(1)–Fe(2)	2.303(3)	S(1)–C(13)	1.646(12)
Fe(1)–Fe(2)	2.618(3)	S(3)–C(13)	1.682(12)
C(13)-Fe(1)-S(2)	83.4(3)	Fe(2)-S(2)-Fe(1)	71.32(11)
S(2)-Fe(1)-Fe(2)	54.23(10)	Fe(4)-S(6)-Fe(3)	71.13(12)
S(1)-Fe(2)-Fe(1)	76.21(11)	S(1)-C(13)-S(3)	127.2(8)
S(6)-Fe(3)-Fe(4)	54.29(11)	S(1)-C(13)-Fe(1)	113.1(6)
S(5)-Fe(4)-Fe(3)	75.93(10)	S(3)-C(13)-Fe(1)	119.5(7)

Figure 2 shows that the macrocyclic cluster **7d** contains two single-butterfly cluster cores Fe(1)Fe(2)S(2)S(1)C(13) and Fe(3)Fe(4)S(6)S(5)C(22), which are connected by the ether chain C(23)C(24)O(13)C(25)C(26)O(14)C(27)C(28) and a 1,4-dithiomethylbenzene group S(3)C(14)C(15)C(16)C(17)-C(18)C(19)C(20)C(21)S(4); this gives a 23-membered macrocycle. Also, it clearly shows that the ether chain is bonded to S(2) and S(6) of the subcluster cores by equatorial bonds C(28)–S(2) and C(23)–S(6), whereas the 1,4-dithiomethylbenzene group is bound to the subclusters through C(13)–S(3) and C(22)–S(4) bonds in an *endo* mode. The dihedral angles between two butterfly wings in the two subcluster cores are very close (89.2 and 87.7°, respectively) and each of the twelve CO ligands bonded to Fe(1), Fe(2), Fe(3), and Fe(4) are terminal. Although the cavity of the macrocycle is empty, the gap between two host macrocyclic molecules is filled with one molecule of MeOH, which was evidently derived from MeOH-containing solvent used in the crystal growing process.

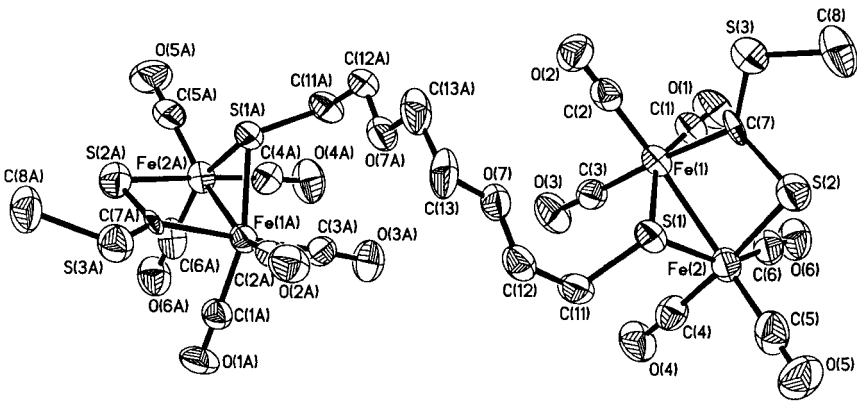

Figure 1. Molecular structure of **6c**.

Reactions of dianions 3 with $[Fe_2(\mu\text{-}S_2)(CO)_6]$/organic halides leading to linear clusters $[\{[Fe_2(CO)_6]_2(\mu\text{-RS})(\mu_4\text{-S})\}_2(\mu\text{-SZS-}\mu)]$ (8a–c) and macrocyclic clusters $[\{[Fe_2(CO)_6]_2(\mu_4\text{-S})\}_2(\mu\text{-SYS-}\mu)(\mu\text{-SZS-}\mu)]$ (9a,b): When an equivalent of $[Fe_2(\mu\text{-}S_2)CO)_6]$ was added to the deep red solution of dianions **3** ($Z = CH_2(CH_2OCH_2)_{1-3}CH_2$), in THF followed by treatment of the intermediate $[Et_3NH]^+$ salts of dianions $[\{[Fe_2(CO)_6]_2$-

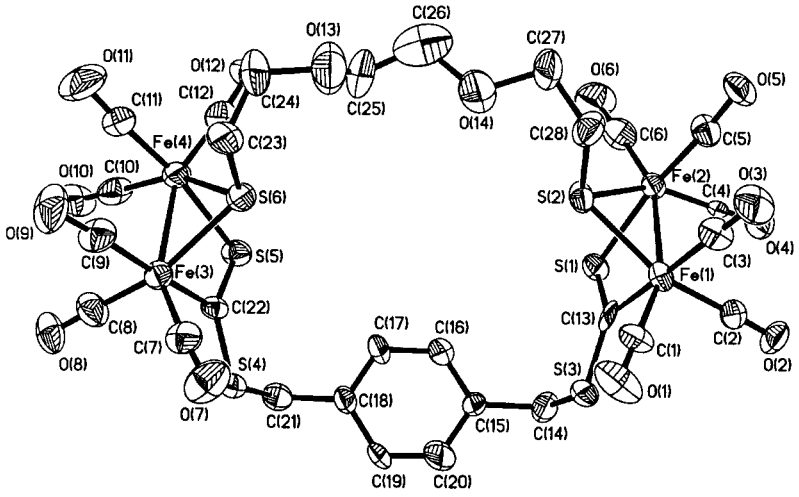

Figure 2. Molecular structure of **7d**.

$(\mu\text{-}S^{-})(\mu_4\text{-}S)\}_2(\mu\text{-}SZS\text{-}\mu)]$ (**n**) with an equivalent or an excess of organic halides, a series of linear clusters **8a–c** and macrocyclic clusters **9a**,**b** were obtained (Scheme 5).

It is noteworthy that the novel type of intermediate sulfur-centered dianions **n** shown in Scheme 5, similar to their analogous sulfur-centered monoanions $[\{Fe_2(CO)_6\}_2(\mu\text{-}RS)(\mu\text{-}S^{-})(\mu_4\text{-}S)]$,[13] were presumably formed by nucleophilic attack by the two negatively charged Fe atoms of anions **3** at one of the S atoms of each $[Fe_2(\mu\text{-}S_2)(CO)_6]$ complex, followed by further coordination of the two resulting μ_3-S atoms to another two Fe atoms and concomitant loss of two μ-CO ligands from intermediate dianions **p** (Scheme 6).

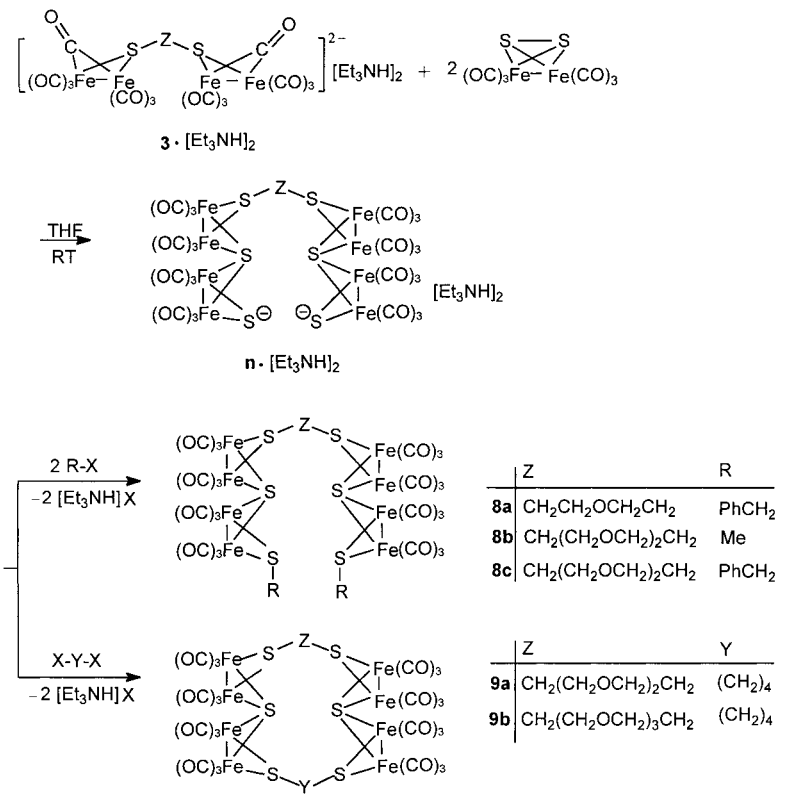

Scheme 5.

New clusters **8a–c** and **9a**,**b** were fully characterized by elemental analysis, and IR and ^{1}H NMR spectroscopic methods. For example, the IR spectra of all the clusters displayed several absorption bands in the range 2098–1985 cm^{-1} for their terminal carbonyl ligands and one band in the region 1121–1109 cm^{-1} for their ether chain functionalities. Since such cluster complexes each contain two μ_4-S atoms, the Z, R, or Y groups should be attached to the bridged μ_2-S atoms by an equatorial type of bond, in order to avoid the strong steric repulsions between R or Z and the axially bonded subcluster core on the μ_4-S atom.[19] This is in good agreement with their ^{1}H NMR spectra, in which all the SCH_2 and MeS groups showed one set of signals at above $\delta = 2$ ppm.[20] This has also been confirmed by X-ray diffraction analysis for **9b** (vide infra).

Crystal structure of 9b: To confirm further the structures of **8a–c** and **9a**,**b**, a single-crystal X-ray diffraction analysis for **9b** was undertaken. The molecular structure of **9b** is shown in Figure 3 and selected bond lengths and angles are presented in Table 2. As can be seen from Figure 3, **9b** is composed of two double-butterfly cluster cores Fe(1)Fe(2)S(1)S(2)-Fe(3)Fe(4)S(3) and Fe(5)-Fe(6)S(4)S(5)Fe(7)Fe(8)S(6) in which S(2) and S(5) atoms are μ_4-S atoms coordinated to the four corresponding iron atoms. In addition, while S(1) and S(4) are bound to C(25) and C(32) of the ether chain $CH_2(CH_2OCH_2)_3CH_2$, S(3) and S(6) atoms are bound to C(33) and C(36) atoms of the butylene group to form a twenty-seven-membered macrocycle. Both the ether chain and the butylene group are indeed connected to the double clusters by an equatorial-type bond, which is necessary to avoid the axial–axial repulsions between the ether chain with the axially bonded subclusters Fe(3)-Fe(4)S(2)S(3) and Fe(7)-Fe(8)S(5)S(6) or the butylene group with subclusters Fe(1)-Fe(2)S(1)S(2) and Fe(5)-Fe(6)S(4)S(5).[19] In addition, each of the twenty four carbonyl groups attached to the eight

0947-6539/03/0901-0174 $ 20.00+.50/0 *Chem. Eur. J.* **2003**, *9*, No. 1

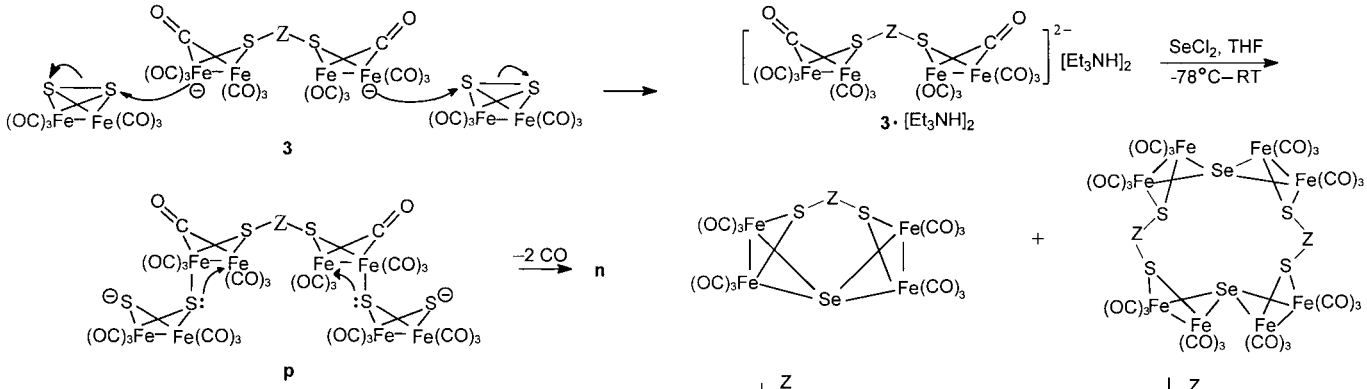

Scheme 6.

	Z
10a*	$(CH_2)_4$
10b*	$CH_2CH_2OCH_2CH_2$
10c*	$CH_2(CH_2OCH_2)_2CH_2$
10d	$CH_2(CH_2OCH_2)_3CH_2$

* were not produced

	Z
11a	$(CH_2)_4$
11b	$CH_2CH_2OCH_2CH_2$
11c	$CH_2(CH_2OCH_2)_2CH_2$
11d	$CH_2(CH_2OCH_2)_3CH_2$

Scheme 7.

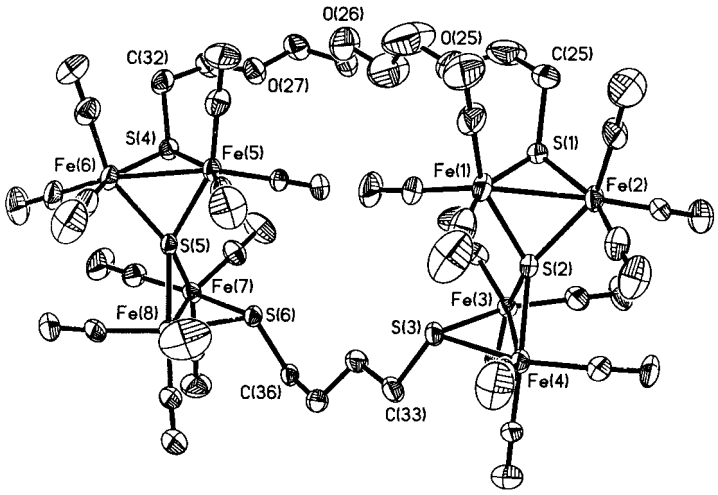

Figure 3. Molecular structure of **9b**.

Table 2. Selected bond lengths [Å] and angles [°] for **9b**.

Fe(1)–S(2)	2.243(3)	Fe(3)–S(3)	2.262(3)
Fe(1)–S(1)	2.258(4)	Fe(3)–Fe(4)	2.537(2)
Fe(1)–Fe(2)	2.542(2)	C(25)–S(1)	1.831(13)
Fe(3)–S(2)	2.238(3)	S(3)–C(33)	1.822(12)
S(2)-Fe(1)-S(1)	76.93(11)	Fe(2)-S(2)-Fe(1)	69.27(10)
S(1)-Fe(1)-Fe(2)	55.68(9)	Fe(4)-S(3)-Fe(3)	68.28(9)
S(2)-Fe(3)-S(3)	76.64(11)	Fe(6)-S(4)-Fe(5)	68.17(10)
S(3)-Fe(3)-Fe(4)	55.79(9)	Fe(6)-S(5)-Fe(8)	133.91(13)
Fe(2)-S(1)-Fe(1)	68.55(11)	Fe(6)-S(5)-Fe(5)	69.16(10)
Fe(3)-S(2)-Fe(4)	68.99(10)	Fe(8)-S(6)-Fe(7)	68.75(10)

iron atoms Fe(1)–Fe(8) are terminal; this is consistent with the spectroscopic data of **9b**.

Reactions of dianions 3 with $SeCl_2$ leading to macrocycles [{$Fe_2(CO)_6$}$_2${μ-$SCH_2(CH_2OCH_2)_3CH_2S$-μ}(μ_4-Se)] (10d) and [{[$Fe_2(CO)_6$]$_2$(μ_4-Se)}$_2$(μ-SZS-μ)$_2$] (11a–d): More interestingly, we also found that when a solution containing an equimolar amount of $SeCl_2$ in THF was added to the solution of the $[Et_3NH]^+$ salts of dianions **3** ($Z = (CH_2)_4$, $CH_2(CH_2OCH_2)_{1-3}CH_2$) in THF at $-78\,^\circ C$ and the mixture stirred at this temperature for 0.5 h then at room temperature for an additional 12 h, the macrocyclic clusters **10d** and **11a–d** were obtained (Scheme 7).

It is worth pointing out that for macrocycles of type **10**, only **10d** ($Z = CH_2(CH_2OCH_2)_3CH_2$) was obtained, that is, **10a–c** ($Z = (CH_2)_4$, $CH_2(CH_2OCH_2)_{1,2}CH_2$) were not able to be produced. Presumably, this is due to the large distortion of the double-butterfly cluster core Fe_4S_2Se in **10a–c** and thus the strains present in these cyclic systems caused by shorter chains $(CH_2)_4$, $CH_2CH_2OCH_2CH_2$, and $CH_2(CH_2OCH_2)_2CH_2$ are too great. In fact, this argument has been supported by X-ray diffraction analysis for **10d**, which showed that the geometry of the double-butterfly core in **10d** is already severely distorted, even though it has a longer ether chain $CH_2(CH_2OCH_2)_3CH_2$ (vide infra).

A possible pathway accounting for the formation of the two types of macrocycles **10d** and **11a–d** is proposed in Scheme 8, on the basis of the well-known chemical reactivity of the one μ-CO-containing monoanions **1**.[4–15] The first step involves a nucleophilic attack by one of either the negatively charged iron atoms of dianions **3** at the selenium in $SeCl_2$ to give intermediate **r**. Then, coordination of the lone electron pair of selenium in **r** to the neighboring iron followed by loss of carbon monoxide gives intermediate **s**. Further repetition of the two steps mentioned above intramolecularly affords macrocycle **10d**. However, if the two steps, namely the nucleophilic attack and the loss of carbon monoxide, take place intermolecularly between two molecules of intermediate **s**, then macrocycles **11a–d** will be formed.

These macrocycles **10d** and **11a–d** are new and have been characterized by combustion analysis, and IR and ^1H NMR spectroscopy. The IR spectra of macrocycles **11a–d** showed three absorption bands in the range $\nu = 2098–1983\ cm^{-1}$ for terminal carbonyl ligands, whereas the IR spectrum of macrocycle **10d** displayed many more (seven) absorption bands in the region $\nu = 2080–1969\ cm^{-1}$ for terminal carbonyl ligands, reflecting the two types of macrocycles. In addition, since the chemical shifts of two SCH_2 in **10d** and four SCH_2 in **11a–d** are in the range $\delta = 2.3–3.0$ ppm, the two terminal CH_2 moieties in the Z group are bound to the bridging S atoms by an equatorial type of bond.[20] In fact, this is consistent with

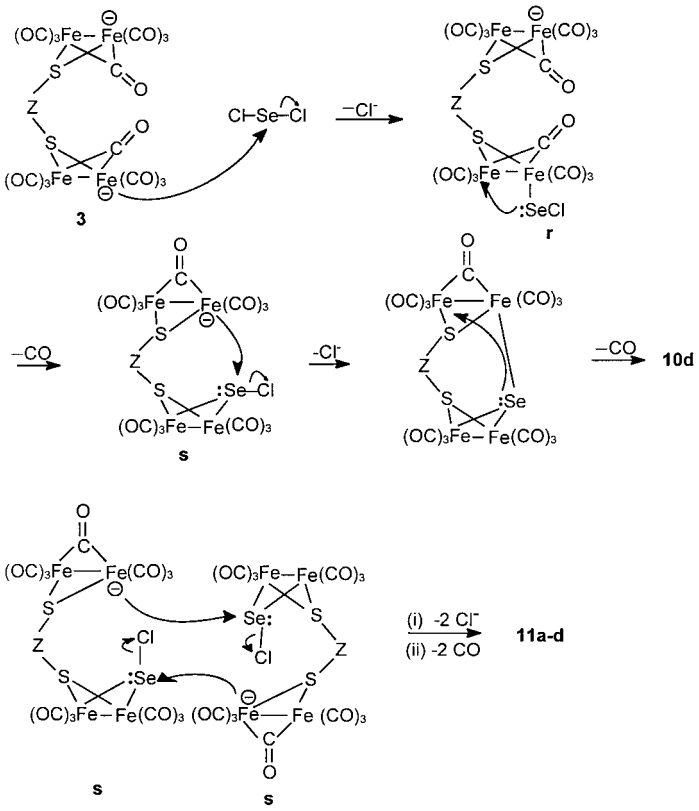

Scheme 8.

other μ_4-S and μ_4-Se-containing butterfly complexes, based on the same reason described above for **8a–c** and **9a**,**b**. In addition, this has been also confirmed by X-ray diffraction analyses for **10d** and **11c** (vide infra).

Crystal structures of 10d and 11c: To unambiguously confirm the two types of macrocyclic cluster complexes, X-ray crystal diffraction studies were performed on complexes **10d** and **11c**. Selected bond lengths and angles are displayed in Table 3 and the molecular structures are depicted in Figures 4 and 5, respectively. Figure 4 shows that **10d** contains a double-butterfly cluster core Fe(1)Fe(2)S(1)Se(1)Fe(3)Fe(4)S(2), which has a spiro type of μ_4-Se(1) coordinated to its four iron atoms. In addition, the double cluster core is bridged by an ether chain through equatorial-type bonds C(13)–S(1) and C(19)–S(2). While each of the iron atoms is bonded to three terminal carbonyl ligands, the two sets of three carbonyls attached to Fe(1) and Fe(2) or Fe(3) and Fe(4) are staggered. This macrocyclic molecule can be formally regarded as derived from a previously reported double cluster complex $[\{Fe_2(\mu\text{-EtS})(CO)_6\}_2(\mu_4\text{-Se})]$[11] by substitution of one β-H atom of each μ-Et group with an ether chain CH_2OCH_2-$CH_2OCH_2CH_2OCH_2$ group. The existence of the ether chain $CH_2(CH_2OCH_2)_3CH_2$ between S(1) and S(2) in macrocyclic compound **10d** has caused apparent changes in parameters of the double cluster core Fe_4S_2Se in $[\{Fe_2(\mu\text{-EtS})(CO)_6\}_2$-$(\mu_4\text{-Se})]$, for example, the average bond length of the four Fe–Se bonds in **10d** (2.3795 Å) is greater than that in $[\{Fe_2(\mu\text{-EtS})(CO)_6\}_2(\mu_4\text{-Se})]$ (2.3568 Å), the average bond lengths of the two Fe–Fe bonds in **10d** (2.5546 Å) are shorter

Table 3. Selected bond lengths [Å] and angles [°] for **10d** and **11c**.

Complex **10d**			
Fe(1)–S(1)	2.2651(13)	Fe(3)–Se(1)	2.3867(9)
Fe(1)–Fe(2)	2.5557(10)	Fe(3)–Fe(4)	2.5535(10)
Fe(2)–S(1)	2.2677(13)	Fe(4)–S(2)	2.2768(13)
Fe(3)–S(2)	2.2586(13)	Fe(1)–Se(1)	2.3831(10)
Fe(2)–Se(1)	2.3754(9)	Fe(4)–Se(1)	2.3729(9)
S(2)-Fe(3)-Se(1)	75.11(3)	Se(1)-Fe(4)-Fe(3)	57.82(3)
Se(1)-Fe(1)-Fe(2)	57.37(3)	S(1)-Fe(1)-Fe(2)	55.73(4)
S(2)-Fe(4)-Se(1)	75.05(3)	Fe(4)-Se(1)-Fe(2)	149.52(3)
S(1)-Fe(1)-Se(1)	74.66(4)	Fe(2)-Se(1)-Fe(1)	64.97(2)
S(2)-Fe(4)-Fe(3)	55.40(3)	Fe(1)-S(1)-Fe(2)	68.64(4)
Se(1)-Fe(2)-Fe(1)	57.66(3)	Fe(1)-Se(1)-Fe(3)	120.95(3)
Complex **11c**			
Fe(1)–Se(1)	2.3438(13)	Fe(1)–S(1)	2.259(2)
Fe(3)–Se(1)	2.3571(13)	Fe(1)–Fe(2)	2.5886(14)
Fe(2)–Se(1)	2.3661(13)	Fe(2)–S(1)	2.268(2)
Fe(4)–Se(1)	2.3582(12)	Fe(3)–S(2)	2.256(2)
Fe(4)–S(2)	2.262(2)	Fe(3)–Fe(4)	2.5639(14)
Fe(1)-Se(1)-Fe(3)	136.14(5)	Se(1)-Fe(2)-Fe(1)	56.25(4)
Fe(3)-Se(1)-Fe(4)	65.88(4)	S(2)-Fe(3)-Se(1)	76.74(6)
Fe(1)-Se(1)-Fe(2)	66.68(4)	Se(1)-Fe(3)-Fe(4)	57.08(4)
S(1)-Fe(1)-Se(1)	77.80(5)	S(2)-Fe(4)-Se(1)	76.60(6)
S(1)-Fe(1)-Fe(2)	55.29(5)	Se(1)-Fe(4)-Fe(3)	57.04(4)
Se(1)-Fe(1)-Fe(2)	57.07(4)	S(1)-Fe(2)-Se(1)	77.16(6)

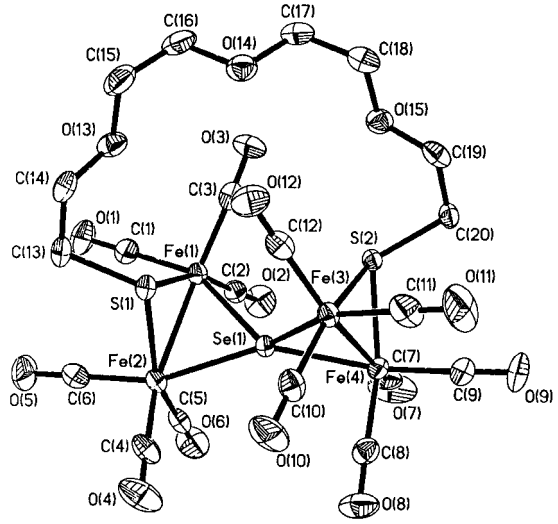

Figure 4. Molecular structure of **10d**.

than that in $[\{Fe_2(\mu\text{-EtS})(CO)_6\}_2(\mu_4\text{-Se})]$ (2.571 Å), and the average bond angle of two Fe-Se-Fe bond angles in **10d** (64.93°) is smaller than that in $[\{Fe_2(\mu\text{-EtS})(CO)_6\}_2(\mu_4\text{-Se})]$ (66.15°). Cluster **11c** is a centrosymetrical molecule and consists of two double-butterfly cluster cores Fe(1)Fe(2)S(1)-Se(1)Fe(3)Fe(4)S(2) and Fe(1A)Fe(2A)S(1A)Se(1A)-Fe(3A)Fe(4A)S(2A), which have two μ_4-Se atoms, that is, Se(1) and Se(1A). In addition, the two ether chains $CH_2(CH_2OCH_2)_2CH_2$ are bridged through equatorial-type bonds C(13)–S(1), C(13A)–S(2A), C(16)–S(2) and C(16A)–S(1A) to the double cluster cores to form a 26-membered macrocycle. Interestingly, similar to those described above for **10d** and $[\{Fe_2(\mu\text{-EtS})(CO)_6\}_2(\mu_4\text{-Se})]$,[11] the geometric parameters of the double-cluster core Fe_4S_2Se in **11c** are different from corresponding those in **10d**. For example, the average bond length of the four Fe–Se bonds in

0947-6539/03/0901-0176 $ 20.00+.50/0 *Chem. Eur. J.* **2003**, *9*, No. 1

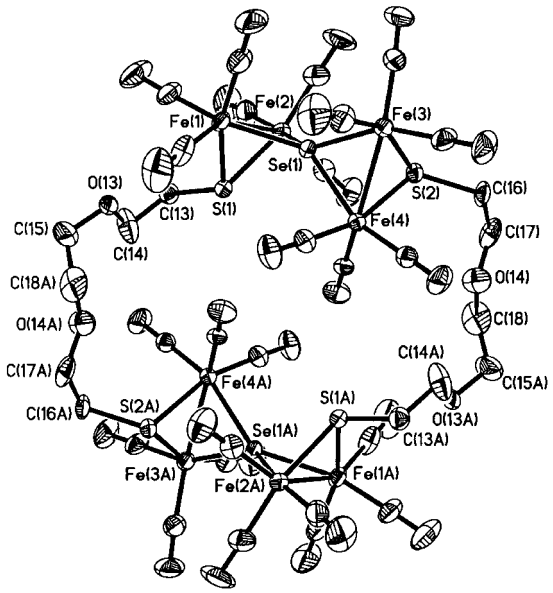

Figure 5. Molecular structure of **11c**.

one double cluster core of **11c** (2.3563 Å) is smaller than that in **10d** (2.3795 Å), the average bond length of the corresponding two Fe–Fe bonds in **11c** (2.5763 Å) is longer than that in **10d** (2.5546 Å), and the average bond angle of the corresponding two Fe-Se-Fe bond angles in **11c** (66.28°) is larger than that in **10d** (64.93°). It follows that while the geometry of the double-butterfly cluster core Fe_4S_2Se in **11c** is essentially not distorted when compared with $[\{Fe_2(\mu\text{-EtS})(CO)_6\}_2(\mu_4\text{-Se})]$,[11] the geometry of Fe_4S_2Se in **10d** is severely distorted, evidently due to the presence of short chain $CH_2(CH_2OCH_2)_3CH_2$ group between the two bridged S(1) and S(2) atoms. So, it is reasonable that we could not obtain the analogues of **10d**, namely **10a–c**, in which the shorter chains $(CH_2)_4$, $CH_2CH_2OCH_2CH_2$ and $CH_2(CH_2OCH_2)_2CH_2$ would make the double butterfly cluster core Fe_4S_2Se too severely distorted to be formed.

Conclusion

On the basis of our discovery of a new type of double-butterfly complex, $[\{Fe_2(\mu\text{-CO})(CO)_6\}_2(\mu\text{-SZS-}\mu)]^{2-}$ (Z = $(CH_2)_4$, $CH_2(CH_2OCH_2)_{1-3}CH_2$) (**3**), which contains two μ-CO ligands, we have performed a series of studies on the reactions of dianions **3** with several types of electrophiles. Such reactions can be rationalized in terms of their action as double iron-centered nucleophiles and may be divided into three classes according to the type of electrophile employed. In one class, reactions with the electrophiles having one leaving group such as PhC(O)Cl or Ph_2PCl produced neutral linear clusters of types $[\{Fe_2(\mu\text{-PhCO})(CO)_6\}_2(\mu\text{-SZS-}\mu)]$ (**4**) and $[\{Fe_2(\mu\text{-Ph}_2P)(CO)_6\}_2(\mu\text{-SZS-}\mu)]$ (**5**) in which the organic groups PhC=O and Ph_2P replaced the two μ-CO ligands. In the second class, reactions with the electrophiles that have no leaving group such as CS_2 and $[Fe_2(\mu\text{-S})_2(CO)_6]$ initially gave the other dianions and finally through subsequent treatment with mono- and dihalides gave both linear and macrocyclic clusters $[\{Fe_2(\mu\text{-RCS}_2)(CO)_6\}_2(\mu\text{-SZS-}\mu)]$ (**6**), $[\{Fe_2(CO)_6\}_2(\mu\text{-SZS-}\mu)(\mu\text{-CS}_2\text{YCS}_2\text{-}\mu)]$ (**7**), $[\{[Fe_2(CO)_6]_2(\mu\text{-RS})(\mu_4\text{-S})\}_2(\mu\text{-SZS-}\mu)]$ (**8**), and $[\{[Fe_2(CO)_6]_2(\mu_4\text{-S})\}_2(\mu\text{-SYS-}\mu)(\mu\text{-SZS-}\mu)]$ (**9**). The third class involves the reactions of dianions **3** with the electrophile containing two leaving groups, that is, $SeCl_2$ to afford neutral macrocyclic clusters $[\{Fe_2(CO)_6\}_2(\mu_4\text{-Se})(\mu\text{-SZS-}\mu)]$ (**10**) and $[\{[Fe_2(CO)_6]_2(\mu_4\text{-Se})\}_2(\mu\text{-SZS-}\mu)_2]$ (**11**). It is believed that in view of the novel reactivities of dianions **3** and the unique structures and properties of the linear and macrocyclic clusters **4–11** (which can be regarded as special types of acyclic and macrocyclic cluster crown ethers) this study will play an important role in further development of both butterfly Fe/E cluster chemistry[4–16] and crown ether supramolecular chemistry.[23]

Experimental Section

General comments: All reactions were carried out under an atmosphere of prepurified nitrogen by using standard Schlenk and vacuum-line techniques. Tetrahydrofuran (THF) was distilled from Na/benzophenone ketyl under nitrogen. $[Fe_2(\mu\text{-S}_2)(CO)_6]$,[20] $[Fe_3(CO)_{12}]$,[24] $HSCH_2(CH_2OCH_2)_nCH_2SH$ ($n = 1-3$),[25, 26] Ph_2PCl,[27] 1,3,5-$Me(BrCH_2)_2C_6H_3$,[28] 1,4-$(BrCH_2)C_6H_4$,[29] $I(CH_2)_4I$,[30] $CpFe(CO)_2I$,[31] and $SeCl_2$[32] were prepared according to literature procedures. PhC(O)Cl, CS_2, MeI, $PhCH_2Br$, Et_3N, and $Br(CH_2)_nBr$ ($n = 2-4$) were of commercial origin and used without further purification. Preparative TLC was carried out on glass plates ($26 \times 20 \times 0.25$ cm) coated with silica gel H (10–40 μm). IR spectra were recorded on a Nicolet Magna 560 FTIR or a Bruker Vector 22 infrared spectrophotometer. ^1H (^{13}C, ^{31}P) NMR spectra were recorded on a Bruker AC-P200 NMR spectrometer. C/H analysis was performed on an Elementar Vario EL analyzer. Melting points were determined on a Yanaco MP-500 apparatus and were uncorrected.

Standard in situ preparation of intermediate salts $[\{Fe_2(\mu\text{-CO})(CO)_6\}_2(\mu\text{-SZS-}\mu)][Et_3NH]_2$ ($3[Et_3NH]_2$): A three-necked flask (100 mL) equipped with a magnetic stir-bar, a rubber septum, and a nitrogen inlet tube was charged with $[Fe_3(CO)_{12}]$ (1.00 g, 1.98 mmol), THF (30 mL), HSZSH [Z = $CH_2CH_2CH_2CH_2$, $CH_2(CH_2OCH_2)_nCH_2 (n = 1-3)$] (1.0 mmol) and Et_3N (0.28 mL, 2.0 mmol). The mixture was stirred at room temperature for 45 min to give a brown-red solution of the intermediate salts $\mathbf{3}\cdot[Et_3NH]_2$ (ca. 1 mmol), which were utilized immediately in the following preparations.

Preparation of $[\{Fe_2(\mu\text{-PhCO})(CO)_6\}_2\{\mu\text{-SCH}_2(CH_2OCH_2)_2CH_2S\text{-}\mu\}]$ (4a): PhCOCl (0.54 mL, 4.65 mmol) was added to the above-prepared solution of $\mathbf{3}[Et_3NH]_2$ ($Z = CH_2(CH_2OCH_2)_2CH_2$), and the mixture stirred at room temperature for 20 h. Solvent was removed under reduced pressure. The residue was subjected to TLC separation using CH_2Cl_2/petroleum ether (v/v = 1:2) as eluent. From the main red band **4a** was obtained as a red oil. Yield: 0.301 g, 32%; ^1H NMR (200 MHz, $CDCl_3$, TMS): $\delta = 2.85$ (br s, 4H; $2SCH_2$), 3.79 (br s, 8H; $4OCH_2$), 7.46 ppm (br s, 10H; $2C_6H_5$); ^{13}C NMR (50 MHz, $CDCl_3$, TMS): $\delta = 38.2$ (s; SCH_2), 70.5 and 71.6 (2s; OCH_2), 126.9, 127.1, 128.2, 128.5 (all s; C_6H_5), 133.3 (s; C_6H_5), 144.4 (s; *ipso*-C_6H_5), 207.4, 209.0, 209.3, 209.8, 211.2, 211.9 (all s; Fe–CO), 289.0 ppm (s, acyl C=O); IR (KBr): $\tilde{\nu} = 2074$, 2032, 1995 (C≡O), 1467 (C=O); 1115 cm^{-1} (C-O-C); elemental analysis calcd (%) for $C_{32}H_{22}Fe_4O_{16}S_2$ (950.0): C 40.46, H 2.34; found C 40.45, H 2.38.

Preparation of $[\{Fe_2(\mu\text{-PhCO})(CO)_6\}_2\{\mu\text{-SCH}_2(CH_2OCH_2)_3CH_2S\text{-}\mu\}]$ (4b): The same procedure was followed as for **4a**, but $\mathbf{3}[Et_3NH]_2$ ($Z = CH_2(CH_2OCH_2)_3CH_2$) was used instead of $\mathbf{3}[Et_3NH]_2$ ($Z = CH_2(CH_2OCH_2)_2CH_2$). From the main red band **4b** was obtained as a red oil. Yield: 0.318 g, 32%; ^1H NMR (200 MHz, $CDCl_3$, TMS): $\delta = 2.80$ (br s, 4H; $2SCH_2$), 3.73 (br s, 12H; $6OCH_2$), 7.43 ppm (br s, 10H; $2C_6H_5$); ^{13}C NMR (50 MHz, $CDCl_3$, TMS): $\delta = 38.2$ (s; SCH_2), 70.4 and 71.7 (2s; OCH_2), 127.1, 128.2 (2s; C_6H_5), 133.3 (s; C_6H_5), 144.4 (s; *ipso* C_6H_5), 208.6, 209.3, 211.2, 211.8, 212.0 (all s; Fe–CO), 289.0 ppm (s; acyl C=O); IR (KBr): $\tilde{\nu} = 2074$, 2032, 1995 (C≡O), 1467 (C=O), 1116 cm^{-1} (C-O-C);

elemental analysis calcd (%) for $C_{34}H_{26}Fe_4O_{17}S_2$ (994.1): C 41.08, H 2.64; found C 41.10, H 2.57.

Preparation of [{Fe$_2$(μ-Ph$_2$P)Fe$_2$(CO)$_6$}$_2$(μ-SCH$_2$(CH$_2$OCH$_2$)$_2$CH$_2$S-μ)] (5a): Ph_2PCl (0.45 g, 2.0 mmol) was added to the above-prepared solution of **3**$[Et_3NH]_2$ (Z = $CH_2(CH_2OCH_2)_2CH_2$), and the mixture stirred at room temperature for 20 h. Solvent was removed under reduced pressure. The residue was subjected to TLC separation using CH_2Cl_2/petroleum ether (v/v = 2:3) as eluent. From the main red band **5a** was obtained as a red solid. Yield: 0.564 g, 51%; m.p. 39–40°C; ^{1}H NMR (200 MHz, $CDCl_3$, TMS): δ = 2.66 (brs, 4H; $2SCH_2$), 3.59 (brs, 8H; $4OCH_2$), 7.25 ppm (brs, 20H; $4C_6H_5$); ^{31}P NMR (81 MHz, $CDCl_3$, H_3PO_4): δ = 142.3 ppm (s); IR (KBr): $\tilde{\nu}$ = 2059, 2019, 1982 (C≡O), 1098 cm^{-1} (C-O-C); elemental analysis calcd (%) for $C_{42}H_{32}Fe_4O_{14}P_2S_2$ (1110.2): C 45.44, H 2.91; found C 45.40, H 3.00.

Preparation of [{Fe$_2$(μ-Ph$_2$P)(CO)$_6$}$_2$(μ-SCH$_2$(CH$_2$OCH$_2$)$_3$CH$_2$S-μ)] (5b): The same procedure as that for **5a** was followed, but **3**$[Et_3NH]_2$ (Z = $CH_2(CH_2OCH_2)_3CH_2$) was used instead of **3**$[Et_3NH]_2$ (Z = $CH_2(CH_2OCH_2)_2CH_2$). Using CH_2Cl_2/petroleum ether (v/v = 2:3) as eluent from the main red band **5b** was obtained as a red solid. Yield: 0.330 g, 29%; m.p. 44–46°C; ^{1}H NMR (200 MHz, $CDCl_3$, TMS): δ = 2.69 (brs, 4H; $2SCH_2$), 3.59 (brs, 12H; $6OCH_2$), 7.24–7.52 ppm (m, 20H; $4C_6H_5$); ^{31}P NMR (81 MHz, $CDCl_3$, H_3PO_4): δ = 142.4 ppm (s); IR (KBr): $\tilde{\nu}$ = 2059, 2019, 1982 (C≡O), 1099 cm^{-1} (C-O-C); elemental analysis calcd (%) for $C_{44}H_{36}Fe_4O_{15}P_2S_2$ (1154.3): C 45.79, H 3.14; found C 45.60, H 3.17.

Preparation of [{Fe$_2$(μ-S=C–SCH$_3$)(CO)$_6$}$_2$(μ-SCH$_2$CH$_2$OCH$_2$CH$_2$S-μ)] (6a): CS_2 (0.24 mL, 4.0 mmol) was added to the above-prepared solution of **3**$[Et_3NH]_2$ (Z = $CH_2CH_2OCH_2CH_2$), and the mixture stirred at room temperature for approximately 30 min. CH_3I (0.25 mL, 4.0 mmol) was added, and then the new mixture stirred at room temperature for 12 h. Solvent was removed under reduced pressure. The residue was subjected to TLC separation with CH_2Cl_2/petroleum ether (v/v = 1:3) as eluent. From the main red band **6a** was obtained as a red solid. Yield: 0.510 g, 58%; m.p. 121–124°C; ^{1}H NMR (200 MHz, $CDCl_3$, TMS): δ = 2.52 (brs, 6H; $2CH_3$), 2.81 (brs, 4H; $2SCH_2$), 3.83 ppm (brs, 4H; $2CH_2O$); IR (KBr): $\tilde{\nu}$ = 2068, 2026, 2002, 1987, 1965(C≡O), 1115 (C-O-C), 1019 cm^{-1} (C=S); elemental analysis calcd (%) for $C_{20}H_{14}Fe_4O_{13}S_6$ (878.1): C 27.36, H 1.61; found C 27.27, H 1.69.

Preparation of [{Fe$_2$(μ-S=C–SCH$_2$Ph)(CO)$_6$}$_2$(μ-SCH$_2$CH$_2$OCH$_2$CH$_2$S-μ)] (6b): The same procedure as that for **6a** was followed, but $PhCH_2Br$ (0.48 mL, 4.0 mmol) was used instead of CH_3I. By using CH_2Cl_2/petroleum ether (v/v = 1:1) as eluent from the main red band **6b** was obtained as a red solid. Yield: 0.639 g, 62%; m.p. 72–74°C; ^{1}H NMR (200 MHz, $CDCl_3$, TMS): δ = 2.83 (brs, 4H; $2SCH_2$), 3.82 (brs, 4H; $2CH_2O$), 4.28 (brs, 4H; $2CH_2Ph$), 7.24 ppm (s, 10H; $2C_6H_5$); IR (KBr): $\tilde{\nu}$ = 2074, 2018, 1985, 1962 (C≡O), 1113 (C-O-C), 1014 cm^{-1} (C=S); elemental analysis calcd (%) for $C_{32}H_{22}Fe_4O_{13}S_6$ (1030.3): C 37.30, H 2.15; found C 37.45, H 2.30.

Preparation of [{Fe$_2$(μ-S=C–SCH$_3$)(CO)$_6$}$_2$(μ-SCH$_2$(CH$_2$OCH$_2$)$_2$CH$_2$S-μ)] (6c): The same procedure as that for **6a** was followed, but **3**$[Et_3NH]_2$ (Z = $CH_2(CH_2OCH_2)_2CH_2$) was used instead of **3**$[Et_3NH]_2$ (Z = $CH_2CH_2OCH_2CH_2$). By using CH_2Cl_2/petroleum ether (v/v = 1:1) as eluent from the main red band **6c** was obtained as a red solid. Yield: 0.561 g, 61%; m.p. 54–56°C; ^{1}H NMR (200 MHz, $CDCl_3$, TMS): δ = 2.54 (brs, 6H; $2CH_3$), 2.80 (brs, 4H; $2SCH_2$), 3.60–3.95 ppm (m, 8H; $4CH_2O$); IR (KBr): $\tilde{\nu}$ = 2074, 2034, 1985 (C≡O), 1113 (C-O-C), 1010 cm^{-1} (C=S); elemental analysis calcd (%) for $C_{22}H_{18}Fe_4O_{14}S_6$ (922.2): C 28.65, H 1.97; found C 28.85, H 2.05.

Preparation of [{Fe$_2$(μ-S=C–SCH$_2$Ph)(CO)$_6$}$_2$(μ-SCH$_2$(CH$_2$OCH$_2$)$_2$CH$_2$S-μ)] (6d): The same procedure as that for **6a** was followed, but **3**$[Et_3NH]_2$ (Z = $CH_2(CH_2O\ CH_2)_2CH_2$) and $PhCH_2Br$ (0.48 mL, 4.0 mmol) were used instead of **3**$[Et_3NH]_2$ (Z = $CH_2CH_2OCH_2CH_2$) and CH_3I, respectively. By using CH_2Cl_2/petroleum ether (v/v = 1:1) as eluent from the main red band **6d** was obtained as a red solid. Yield: 0.700 g, 65%; m.p. 110–112°C; ^{1}H NMR (200 MHz, $CDCl_3$, TMS): δ = 2.80 (brs, 4H; $2SCH_2$), 3.70–3.95 (m, 8H; $4CH_2O$), 4.29 (s, 4H; $2CH_2Ph$), 7.25 ppm (brs, 10H; $2C_6H_5$); IR (KBr): $\tilde{\nu}$ = 2066, 2026, 2001, 1979 (C≡O), 1115 (C-O-C), 1014 cm^{-1} (C=S); elemental analysis calcd (%) for $C_{34}H_{26}Fe_4O_{14}S_6$ (1074.4): C 38.01, H 2.44; found C 37.64, H 2.42.

Preparation of [{Fe$_2$(CO)$_6$[μ-S=C–SFeCp(CO)$_2$]}$_2$}{μ-SCH$_2$-(CH$_2$OCH$_2$)$_2$CH$_2$S-μ] (6e): The same procedure as that for **6a** was followed, but **3**$[Et_3NH]_2$ (Z = $CH_2(CH_2OCH_2)_2CH_2$) and $[FeCp(CO)_2I]$ (0.608 g, 2.0 mmol) were used instead of **3**$[Et_3NH]_2$ (Z = $CH_2CH_2OCH_2CH_2$) and CH_3I, respectively. By using CH_2Cl_2/petroleum ether (v/v = 2:1) as eluent from the main red band **6e** was obtained as a red solid. Yield: 0.650 g, 52%; m.p. 82–84°C; ^{1}H NMR (200 MHz, $CDCl_3$, TMS): δ = 2.72 (brs, 4H; $2SCH_2$), 3.72 (brs, 8H; $4CH_2O$), 4.96 ppm (s, 10H; $2C_5H_5$); IR (KBr): $\tilde{\nu}$ = 2058, 2018, 1977 (C≡O), 1121 (C-O-C), 1002 cm^{-1} (C=S); elemental analysis calcd (%) for $C_{34}H_{22}Fe_6O_{18}S_6$ (1246.0): C 32.77, H 1.78; found C 32.65, H 1.80.

Preparation of [{Fe$_2$(CO)$_6$}$_2${μ-S(CH$_2$)$_4$S-μ}{μ-S=C–S-1-CH$_2$(3-MeC$_6$H$_3$)-CH$_2$-5-S–C=S-μ}] (7a): CS_2 (0.24 mL, 4.0 mmol) was added to the above-prepared solution of **3**$[Et_3NH]_2$ (Z = $CH_2CH_2CH_2CH_2$), and the mixture stirred at room temperature for approximately 30 min. 1,3,5-$Me(CH_2Br)_2C_6H_3$ (0.278 g, 1.0 mmol) was added and then the new mixture stirred at room temperature for 12 h. Solvent was removed under reduced pressure. The residue was subjected to TLC separation using CH_2Cl_2/petroleum ether (v/v = 1:2) as eluent. From the main red band **7a** was obtained as a red solid. Yield: 0.140 g, 15%; m.p. 117–119°C; ^{1}H NMR (200 MHz, $CDCl_3$, TMS): δ = 2.06 (brs, 4H; CH_2CH_2), 2.28 (s, 3H; CH_3), 2.64 (brs, 4H; $2SCH_2$), 4.23 (s, 4H; $2CH_2Ar$), 6.96 ppm (brs, 3H; C_6H_3); IR (KBr): $\tilde{\nu}$ = 2074, 2026, 1985 (C≡O), 1014 cm^{-1} (C=S); elemental analysis calcd (%) for $C_{27}H_{18}Fe_4O_{12}S_6$ (950.2): C 34.13, H 1.91; found C 33.78, H 1.99.

Preparation of [{Fe$_2$(CO)$_6$}$_2$(μ-SCH$_2$CH$_2$OCH$_2$CH$_2$S-μ){μ-S=C–S-(CH$_2$)$_2$S–C=S-μ}] (7b): The same procedure as that for **7a** was followed, but **3**$[Et_3NH]_2$ (Z = $CH_2CH_2OCH_2CH_2$) and $BrCH_2CH_2Br$ (0.09 mL, 1.0 mmol) were used instead of **3**$[Et_3NH]_2$ (Z = $CH_2CH_2CH_2CH_2$) and 1,3,5-$Me(CH_2Br)_2C_6H_3$, respectively. From the main red band **7b** was obtained as a red solid. Yield: 0.110 g, 13%; m.p. 191°C (decomp); ^{1}H NMR (200 MHz, $CDCl_3$, TMS): δ = 1.59 (s, 4H; SCH_2CH_2S), 2.55–3.10 (m, 4H; $2SCH_2$), 3.60–4.05 ppm (m, 4H; $2CH_2O$); IR (KBr): $\tilde{\nu}$ = 2064, 2024, 2002, 1979 (C≡O), 1120 (C-O-C), 1013 cm^{-1} (C=S); elemental analysis calcd (%) for $C_{20}H_{12}Fe_4O_{13}S_6$ (876.1): C 27.42, H 1.38; found C 27.75, H 1.40.

Preparation of [{Fe$_2$(CO)$_6$}$_2${μ-SCH$_2$(CH$_2$OCH$_2$)$_2$CH$_2$S-μ}{μ-S=C–S-(CH$_2$)$_3$S–C=S-μ}] (7c): The same procedure as that for **7a** was followed, but **3**$[Et_3NH]_2$ (Z = CH_2 $(CH_2OCH_2)_2CH_2$) and $Br(CH_2)_3Br$ (0.10 mL, 1.0 mmol) were used instead of **3**$[Et_3NH]_2$ (Z = $CH_2CH_2CH_2CH_2$) and 1,3,5-$Me(CH_2Br)_2C_6H_3$, respectively. By using CH_2Cl_2/petroleum ether (v/v = 2:1) as eluent from the main red band **7c** was obtained as a red solid. Yield: 0.150 g, 16%; m.p. 135°C (decomp); ^{1}H NMR (200 MHz, $CDCl_3$, TMS): δ = 1.86 (s, 2H; $SCH_2CH_2CH_2S$), 2.60–3.05 (m, 8H; $4SCH_2$), 3.75–4.05 ppm (m, 8H; $4CH_2O$); IR (KBr): $\tilde{\nu}$ = 2074, 2026, 1989, 1970 (C≡O), 1105 (C-O-C), 1014 cm^{-1} (C=S); elemental analysis calcd (%) for $C_{23}H_{18}Fe_4O_{14}S_6$ (934.2): C 29.57, H 1.94; found C 29.28, H 1.89.

Preparation of [{Fe$_2$(CO)$_6$}$_2${μ-SCH$_2$(CH$_2$OCH$_2$)$_2$CH$_2$S-μ}{μ-S=C–S-1-CH$_2$C$_6$H$_4$CH$_2$-4-S–C=S-μ}] (7d): The same procedure as that for **7a** was followed, but **3**$[Et_3NH]_2$ (Z = $CH_2(CH_2OCH_2)_2CH_2$) and 1,4-$(BrCH_2)_2C_6H_4$ (0.26 g, 1.0 mmol) were used instead of **3**$[Et_3NH]_2$ (Z = $CH_2CH_2CH_2CH_2$) and 1,3,5-$Me(CH_2Br)_2C_6H_3$, respectively. By using CH_2Cl_2/petroleum ether (v/v = 3:2) as eluent from the main red band **7d** was obtained as a red solid. Yield: 0.144 g, 15%; m.p. 104–106°C; ^{1}H NMR (200 MHz, $CDCl_3$, TMS): δ = 2.81 (brs, 4H; $2SCH_2$), 3.72–3.85 (m, 8H; $4CH_2O$), 4.20–4.45 (m, 4H; $2SCH_2Ar$), 7.15 ppm (s, 4H; C_6H_4); IR (KBr): $\tilde{\nu}$ = 2074, 2018, 1981 (C≡O), 1105 (C-O-C), 1014 cm^{-1} (C=S); elemental analysis calcd (%) for $C_{28}H_{20}Fe_4O_{14}S_6$ (996.2): C 33.76, H 2.02; found C 33.68, H 2.05.

Preparation of [{Fe$_2$(CO)$_6$}$_2$(μ-SCH$_2$(CH$_2$OCH$_2$)$_3$CH$_2$S-μ}{μ-S=C–S-(CH$_2$)$_4$S–C=S-μ}] (7e): The same procedure as that for **7a** was followed, but **3**$[Et_3NH]_2$ (Z = $CH_2(CH_2OCH_2)_3CH_2$) and $I(CH_2)_4I$ (0.13 mL, 1.0 mmol) were used instead of **3**$[Et_3NH]_2$ (Z = $CH_2CH_2CH_2CH_2$) and 1,3,5-$Me(CH_2Br)_2C_6H_3$, respectively. By using CH_2Cl_2/petroleum ether (v/v = 2:1) as eluent from the main red band **7e** was obtained as a red solid. Yield: 0.110 g, 11%; m.p. 107–108°C; ^{1}H NMR (200 MHz, $CDCl_3$, TMS): δ = 1.68 (brs, 4H; $SCH_2CH_2CH_2CH_2S$), 2.80 (brs, 8H; $4SCH_2$), 3.65–4.05 ppm (m, 12H; $6CH_2O$); IR (KBr): $\tilde{\nu}$ = 2066, 2024, 1993 (C≡O), 1107 (C-O-C), 1017 cm^{-1} (C=S); elemental analysis calcd (%) for $C_{26}H_{24}Fe_4O_{15}S_6$ (992.3): C 31.47, H 2.44; found C 31.79, H 2.30.

Preparation of [{[Fe$_2$(CO)$_6$}$_2$(μ-SCH$_2$C$_6$H$_5$)(μ_4-S)}$_2$(μ-SCH$_2$CH$_2$-OCH$_2$CH$_2$S-μ)] (8a): [$Fe_2(\mu$-$S_2)(CO)_6$] (0.688 g, 2.0 mmol) was added to the above prepared solution of **3**$[Et_3NH]_2$ (Z = $CH_2CH_2OCH_2CH_2$), and the mixture was stirred at room temperature for approximately 2 h. To this mixture was added $PhCH_2Br$ (0.48 mL, 4.0 mmol), and the new mixture

0947-6539/03/0901-0178 $ 20.00+.50/0 *Chem. Eur. J.* **2003**, *9*, No. 1

was stirred at room temperature for 24 h. Solvent was removed under reduced pressure. The residue was subjected to TLC separation using CH_2Cl_2/petroleum ether (v/v = 1:2) as eluent. From the main red band **8a** was obtained as a red solid. Yield: 0.500 g, 32%; m.p. 66–68 °C; ^{1}H NMR (200 MHz, $CDCl_3$, TMS): $\delta = 2.61$ (s, 4H; $2SCH_2$), 3.55–3.80 (m, 8H; $2CH_2O$, $2PhCH_2$), 7.32 ppm (s, 10H; $2C_6H_5$); IR (KBr): $\tilde{\nu} = 2090$, 2034, 1985 (C≡O), 1113 cm^{-1} (C-O-C); elemental analysis calcd (%) for $C_{42}H_{22}Fe_8O_{25}S_6$ (1565.8): C 32.22, H 1.42; found C 32.34, H 1.89.

Preparation of [[Fe$_2$(CO)$_6$]$_2$(μ-SCH$_3$)(μ_4-S)}$_2${μ-SCH$_2$(CH$_2$OCH$_2$)$_2$CH$_2$-S-μ}] (8b): The same procedure as that for **8a** was followed, but **3**[Et$_3$NH]$_2$ (Z = $CH_2(CH_2OCH_2)_2CH_2$) and CH_3I (0.25 mL, 4.0 mmol) were used instead of **3**[Et$_3$NH]$_2$ (Z = $CH_2CH_2OCH_2CH_2$) and $PhCH_2Br$, respectively. By using CH_2Cl_2/petroleum ether (v/v = 1:1) as eluent from the main red band **8b** was obtained as a red solid. Yield: 0.450 g, 31%; m.p. 66 °C (decomp); ^{1}H NMR (200 MHz, $CDCl_3$, TMS): $\delta = 2.14$ (brs, 6H; $2CH_3$), 2.62 (brs, 4H; $2SCH_2$), 3.68 ppm (brs, 8H; $4CH_2O$); IR (KBr): $\tilde{\nu} = 2098$, 2042, 1989 (C≡O), 1109 cm^{-1} (C-O-C); elemental analysis calcd (%) for $C_{32}H_{18}Fe_8O_{26}S_6$ (1457.7): C 26.37, H 1.24; found C 26.41, H 1.37.

Preparation of [{[Fe$_2$(CO)$_6$]$_2$(μ-SCH$_2$C$_6$H$_5$)(μ_4-S)}$_2${μ-SCH$_2$(CH$_2$OCH$_2$)$_2$-CH$_2$S-μ}] (8c): The same procedure as that for **8a** was followed, but **3**[Et$_3$NH]$_2$ (Z = $CH_2(CH_2OCH_2)_2CH_2$) was used instead of **3**[Et$_3$NH]$_2$ (Z = $CH_2CH_2OCH_2CH_2$). By using CH_2Cl_2/petroleum ether (v/v = 1:1) as eluent from the main red band **8c** was obtained as a red solid. Yield: 0.610 g, 38%; m.p. 84–86 °C; ^{1}H NMR (200 MHz, $CDCl_3$, TMS): $\delta = 2.63$ (brs, 4H; $2SCH_2$), 3.65 (brs, 12H; $4CH_2O$, $2CH_2Ph$), 7.33 ppm (brs, 10H; $2C_6H_5$); IR (KBr): $\tilde{\nu} = 2090$, 2042, 1985 (C≡O), 1109 cm^{-1} (C-O-C); elemental analysis calcd (%) for $C_{44}H_{26}Fe_8O_{26}S_6$ (1609.9): C 32.83, H 1.63; found C 32.64, H 1.71.

Preparation of [{[Fe$_2$(CO)$_6$]$_2$(μ_4-S)}$_2${μ-SCH$_2$(CH$_2$OCH$_2$)$_2$CH$_2$S-μ}-{μ-S(CH$_2$)$_4$S-μ}] (9a): [Fe$_2$(μ-S$_2$)(CO)$_6$] (0.688 g, 2.0 mmol) was added to the above-prepared solution of **3**[Et$_3$NH]$_2$ (Z = $CH_2(CH_2OCH_2)_2CH_2$), and the mixture stirred at room temperature for approximately 2 h. To this mixture was added I(CH$_2$)$_4$I (0.13 mL, 1.0 mmol) and the new mixture stirred for 24 h. Solvent was removed under reduced pressure. The residue was subjected to TLC separation using CH_2Cl_2/petroleum ether (v/v = 2:1) as eluent. From the main red band **9a** was obtained as a red solid. Yield: 0.240 g, 16%; m.p. 170 °C (decomp); ^{1}H NMR (200 MHz, $CDCl_3$, TMS): $\delta = 1.84$ (brs, 4H; $CH_2CH_2CH_2CH_2$), 2.30–2.85 (m, 8H; $4SCH_2$), 3.55–3.85 ppm(m, 8H; $4CH_2O$); IR (KBr): $\tilde{\nu} = 2084$, 2057, 2034, 1989 (C≡O), 1121 cm^{-1} (C-O-C); elemental analysis calcd (%) for $C_{34}H_{20}Fe_8O_{26}S_6$ (1483.7): C 27.52, H 1.36; found C 27.08, H 1.55.

Preparation of [{[Fe$_2$(CO)$_6$]$_2$(μ_4-S)}$_2${μ-SCH$_2$(CH$_2$OCH$_2$)$_3$CH$_2$S-μ}-{μ-S(CH$_2$)$_4$S-μ}] (9b): The same procedure as that for **9a** was followed, but **3**[Et$_3$NH]$_2$ (Z = $CH_2(CH_2OCH_2)_3CH_2$) was used instead of **3**[Et$_3$NH]$_2$ (Z = $CH_2(CH_2OCH_2)_2CH_2$). From the main red band **9b** was obtained as a red solid. Yield: 0.270 g, 18%; m.p. 210 °C (decomp); ^{1}H NMR (200 MHz, $CDCl_3$, TMS): $\delta = 1.80–2.00$ (m, 4H; $CH_2CH_2CH_2CH_2$), 2.40–2.80 (m, 8H; $4SCH_2$), 3.60–3.83 ppm (m, 12H; $6CH_2O$); IR (KBr): $\tilde{\nu} = 2084$, 2043, 2033, 1987 (C≡O), 1116 cm^{-1} (C-O-C); elemental analysis calcd (%) for $C_{36}H_{24}Fe_8O_{27}S_6$ (1527.7): C 28.30, H 1.58; found C 27.89, H 1.77.

Preparation of [{[Fe$_2$(CO)$_6$]$_2$(μ_4-Se)}$_2${μ-S(CH$_2$)$_4$S-μ}$_2$] (11a): The above-prepared solution of **3**[Et$_3$NH]$_2$ (Z = $CH_2CH_2CH_2CH_2$) was cooled to −78 °C by using an acetone/dry ice bath, and $SeCl_2$ (1 mmol) in THF (5 mL), prepared from Se powder and SO_2Cl_2,[32] was added to this solution. The mixture was stirred for 30 min at −78 °C. After the bath was removed, the mixture was naturally warmed to room temperature and then stirred at this temperature for 12 h. Solvent was removed under reduced pressure and the residue was subjected to TLC separation using CH_2Cl_2/petroleum ether (v/v = 1:1) as eluent. From the main red band **11a** was obtained as a red solid. Yield: 0.100 g, 13%; m.p. 120 °C (decomp); ^{1}H NMR (200 MHz, $CDCl_3$, TMS): $\delta = 1.55–1.80$ (m, 8H; $2CH_2CH_2CH_2CH_2$), 2.30–2.70 ppm (m, 8H; $4SCH_2$); IR (KBr): $\tilde{\nu} =$ 2082, 2034, 1985 cm^{-1} (C≡O); elemental analysis calcd (%) for $C_{32}H_{16}Fe_8O_{24}S_4Se_2$ (1517.4): C 25.32, H 1.06; found C 25.69, H 1.34.

Preparation of [{[Fe$_2$(CO)$_6$]$_2$(μ_4-Se)}$_2${μ-SCH$_2$CH$_2$OCH$_2$CH$_2$S-μ}$_2$] (11b): The same procedure as that for **11a** was followed, but **3**[Et$_3$NH]$_2$ (Z = $CH_2CH_2OCH_2CH_2$) was used instead of **3**·[Et$_3$NH]$_2$ (Z = $CH_2CH_2CH_2CH_2$). From the main red band **11b** was obtained as a red solid. Yield: 0.100 g, 13%; m.p. >300 °C (decomp); ^{1}H NMR (200 MHz, $CDCl_3$, TMS): $\delta = 2.66$ (brs, 8H; $4SCH_2$), 3.75 ppm (brs, 8H; $4CH_2O$); IR (KBr): $\tilde{\nu} = 2098$, 2042, 1989 (C≡O), 1109 cm^{-1} (C-O-C); elemental analysis calcd (%) for $C_{32}H_{16}Fe_8O_{26}S_4Se_2$ (1549.3): C 24.80, H 1.04; found C 25.05, H 1.38.

Table 4. Crystal data and structural refinements retails for **6c**, **7d**, **9b**, **10d**, and **11c**.

	6c	**7d**	**9b**	**10d**	**11c**
formula	$C_{22}H_{18}Fe_4O_{14}S_6 \cdot 2H_2O$	$C_{28}H_{20}Fe_4O_{14}S_6 \cdot 0.5CH_3OH$	$C_{36}H_{24}Fe_8O_{27}S_6 \cdot CH_2Cl_2 \cdot 0.5H_2O$	$C_{20}H_{16}Fe_4O_{15}S_2Se$	$C_{36}H_{24}Fe_8O_{28}S_4Se_2$
M_r	958.16	1012.22	1621.65	862.81	1637.51
T [K]	293(2)	293(2)	293(2)	293(2)	293(2)
crystal system	orthorhombic	triclinic	triclinic	orthorhombic	monoclinic
space group	*Pccn*	$P\bar{1}$	$P\bar{1}$	$P2_12_12_1$	$P2_1/n$
a [Å]	15.171(7)	8.198(3)	12.643(4)	9.792(3)	9.472(2)
b [Å]	17.177(7)	14.912(6)	15.601(6)	16.490(5)	24.863(6)
c [Å]	15.018(6)	19.402(7)	16.768(6)	19.077(5)	13.144(3)
α [°]	90	104.457(8)	82.643(6)	90	90
β [°]	90	97.953(8)	70.777(6)	90	109.995(4)
γ [°]	90	102.998(8)	84.743(7)	90	90
V [Å^3]	3913(3)	2189.7(14)	3093.0(18)	3080.5(15)	2909.0(12)
Z	4	2	2	4	2
ρ [mg m^{-3}]	1.626	1.535	1.741	1.860	1.869
μ [mm^{-1}]	1.834	1.641	2.186	3.228	3.411
crystal size [mm]	0.25 × 0.20 × 0.15	0.25 × 0.20 × 0.15	0.15 × 0.10 × 0.05	0.40 × 0.40 × 0.30	0.20 × 0.20 × 0.15
F(000)	1928	1018	1614	1704	1608
index ranges	$-14 \le h \le 18$	$-9 \le h \le 8$	$-15 \le h \le 8$	$-11 \le h \le 11$	$-11 \le h \le 11$
	$-20 \le k \le 20$	$-17 \le k \le 16$	$-18 \le k \le 18$	$-9 \le k \le 19$	$-22 \le k \le 29$
	$-11 \le l \le 17$	$-19 \le l \le 23$	$-19 \le l \le 19$	$-22 \le l \le 22$	$-15 \le l \le 14$
scan type	*ω-2θ*	*ω-2θ*	*ω-2θ*	*ω* − *2θ*	*ω* − *2θ*
relections collected	15225	8935	12328	12816	11980
independent reflections	3404($R_{int} = 0.2083$)	7520($R_{int} = 0.0581$)	10402($R_{int} = 0.0575$)	5437($R_{int} = 0.0408$)	5145($R_{int} = 0.0585$)
$2\theta_{max}$ [°]	50.06	50.06	50.06	50.06	50.06
data/restraints/parameters	3404/2/226	7520/1/477	10402/12/730	5437/0/380	5145/4/361
R	0.0681	0.0737	0.0688	0.0302	0.0418
Rw	0.1400	0.1197	0.1470	0.0421	0.0878
goooodness of fit	0.888	0.862	0.980	0.928	1.007
largest diff peak/hole [e Å^{-3}]	0.937/−0.361	0.429/−0.355	0.769/−0.561	0.302/−0.433	0.738/−0.547

  0947-6539/03/0901-0179 $ 20.00+.50/0

Preparation of [{[$Fe_2(CO)_6$]$_2$(μ_4-Se)}$_2$(μ-$SCH_2(CH_2OCH_2)_2CH_2S$-μ}$_2$] (11c): The same procedure as that for **11a** was followed, but **3**[Et_3NH]$_2$ (Z = $CH_2(CH_2OCH_2)_2CH_2$) was used instead of **3**[Et_3NH]$_2$ (Z = $CH_2CH_2CH_2CH_2$). From the main red band **11c** was obtained as a red solid. Yield: 0.160 g, 20%; m.p. >300 °C; ^{1}H NMR (200 MHz, $CDCl_3$, TMS): δ = 2.50–2.85 (m, 8H; 4SCH_2), 3.65–3.80 ppm (m, 16H; 8CH_2O); IR (KBr): $\tilde{\nu}$ = 2082, 2033, 1988 (C≡O), 1105 cm^{-1} (C-O-C); elemental analysis calcd (%) for $C_{36}H_{24}Fe_8O_{28}S_4Se_2$ (1637.5): C 26.40, H 1.48; found C 26.55, H 1.43.

Preparation of [{$Fe_2(CO)_6$}$_2$(μ_4-Se){μ-$SCH_2(CH_2OCH_2)_3CH_2S$-μ}] (10d) and [{[$Fe_2(CO)_6$]$_2$(μ_4-Se)}$_2${μ-$SCH_2(CH_2OCH_2)_3CH_2S$-μ}$_2$] (11d): The same procedure as that for **11a** was followed, but **3**[Et_3NH]$_2$ (Z = $CH_2(CH_2OCH_2)_3CH_2$) was used instead of **3**[Et_3NH]$_2$ (Z = $CH_2CH_2CH_2CH_2$). By using CH_2Cl_2/petroleum ether (v/v = 3:2) as eluent from the first main red band **10d** was obtained as a red solid. Yield: 0.070 g, 8%; m.p. >300 °C; ^{1}H NMR (200 MHz, $CDCl_3$, TMS): δ = 2.40–2.95 (m, 4H; 2SCH_2), 3.45–3.90 ppm (m, 12H; 6CH_2O); IR (KBr): $\tilde{\nu}$ = 2080, 2032, 2014, 1995, 1985, 1978, 1969 (C≡O), 1117 cm^{-1} (C-O-C); elemental analysis calcd (%) for $C_{20}H_{16}Fe_4O_{15}S_2Se$ (862.8): C 27.84, H 1.87; found C 27.74, H 1.51.

From the second main red band **11d** was obtained as a red solid. Yield: 0.075 g, 9%; m.p. >300 °C ; ^{1}H NMR (200 MHz, $CDCl_3$, TMS): δ = 2.55–2.80 (m, 8H; 4SCH_2), 3.58–3.90 pmm (m, 24H; 12CH_2O); IR (KBr): $\tilde{\nu}$ = 2082, 2031, 1983 (C≡O), 1119 cm^{-1} (C-O-C); elemental analysis calcd (%) for $C_{40}H_{32}Fe_8O_{30}S_4Se_2$ (1725.6): C 27.84, H 1.87; found C 27.83, H 1.44.

X-ray crystal structure determinations of 6c, 7d, 9b, 10d, and 11c: Single crystals of **6c**, **7d**, **9b**, **10d**, and **11c** suitable for X-ray diffraction analyses were grown by slow evaporation of their CH_2Cl_2/hexane solutions for **6c**, **9b** and **10d**, or the MeOH/hexane solution for **7d**, or EtOH/hexane solution for **11c** at about 4 °C. Each single crystal was mounted on a glass fibre in an arbitrary orientation and determined on a Bruker Smart 1000 automated diffractometer equipped with a graphite monochromated MoKα radiation (λ = 0.71073 Å). The structures of **6c**, **7d**, **9b**, **10d**, and **11c** were solved by direct methods by using the SHELXTL-97 program and refined by full-matrix least-squares on F^2. Hydrogen atoms were located by using the geometric method. All calculations were performed on a Bruker Smart computer. Details of the crystals, data collections, and structure refinements are summarized in Table 4.

CCDC 192686, 174357, 174358, 192687, and 192688 contain the supplementary crystallographic data for **6c**, **7d**, **9b**, **10d** and **11c**, respectively. These data can be obtained free of charge via www.ccdc.cam.ac.uk/conts/retrieving.html (or from the Cambridge Crystallographic Data Centre, 12 Union Road, Cambridge CB2 1EZ, UK; fax: (+44) 1223-336033; or deposit@ccdc.cam.ac.uk).

Acknowledgements

We are grateful to the National Natural Science Foundation of China and the State Key Laboratory of Organometallic Chemistry for financial support of this work.

[1] For reviews, see for example: a) L. Marko', B. Marko'-Monostory in *The Organic Chemistry of Iron, Vol. 2* (Eds.: E. A. K. von Gustorf, F.-W.Grevels, I. Fischler), Academic Press, New York, **1981**, pp. 283–332; b) H. Ogino, S. Inomata, H. Tobita, *Chem. Rev.* **1998**, *98*, 2093–2121; c) L.-C. Song in *Advances in Organometallic Chemistry* (Eds.: Y. Huang, Y. Qian), Chemical Industry Press, Beijing, **1987**, pp. 181–204; d) L.-C. Song, *Trends Organomet. Chem.* **1999**, *3*, 1–20.

[2] a) J. M. Berg, R. H. Holm in *Iron–Sulfur Proteins* (Ed.: T. G. Spiro), Wiley, New York, **1982**, pp. 1–66; b) L. Noodleman, J.-G. Norman, Jr., J. H. Osborne, A. Aizman, D. A. Case, *J. Am. Chem. Soc.* **1985**, *107*, 3418–3426.

[3] a) M. Schmidt, S. M. Contakes, T. B. Rauchfuss, *J. Am. Chem. Soc.* **1999**, *121*, 9736–9737; b) F. Gloaguen, J. D. Lawrence, T. B. Rauchfuss, *J. Am. Chem. Soc.* **2001**, *123*, 9476–9477; c) F. Gloaguen, J. D. Lawrence, M. Schmidt, S. R. Wilson, T. B. Rauchfuss, *J. Am. Chem. Soc.* **2001**, *123*, 12518–12527; d) E. J. Lyon, I. P. Georgakaki, J. H. Reibenspies, M. Y. Darensbourg, *J. Am. Chem. Soc.* **2001**, *123*, 3268–3278.

[4] D. Seyferth, G. B. Womack, J. C. Dewan, *Organometallics* **1985**, *3*, 398–400.

[5] D. Seyferth, J. B. Hoke, J. C. Dewan, *Organometallics* **1987**, *6*, 895–897.

[6] D. Seyferth, D. P. Ruschke, W. M. Davis, M. Cowie, A. D. Hunter, *Organometallics* **1994**, *13*, 3834–3848.

[7] E. Delgado, E. Hernández, O. Rossell, M. Seco, E. G. Puebla, C. Ruiz, *J. Organomet. Chem.* **1993**, *455*, 177–184.

[8] L.-C. Song, Q.-M. Hu, *J. Organomet. Chem.* **1991**, *414*, 219–226.

[9] L.-C. Song, C.-G. Yan, Q.-M. Hu, R.-J. Wang, T. C. W. Mak, *Organometallics* **1995**, *14*, 5513–5519.

[10] L.-C. Song, C.-G. Yan, Q.-M. Hu, B.-M. Wu, T. C. W. Mak, *Organometallics* **1997**, *16*, 632–635.

[11] L.-C. Song, C.-G. Yan, Q.-M. Hu, R.-J. Wang, T. C. W. Mak, X.-Y. Huang, *Organometallics* **1996**, *15*, 1535–1544.

[12] L.-C. Song, H.-T. Fan, Q.-M. Hu, X.-D. Qin, W.-F. Zhu, Y. Chen, J. Sun, *Organometallics* **1998**, *17*, 3454–3459.

[13] L.-C. Song, G.-L. Lu, Q.-M. Hu, H.-T. Fan, Y. Chen, J. Sun, *Organometallics* **1999**, *18*, 3258–3260.

[14] L.-C. Song, G.-L. Lu, Q.-M. Hu, J. Sun, *Organometallics* **1999**, *18*, 5429–5431.

[15] L.-C. Song, G.-L. Lu, Q.-M. Hu, J. Sun, *Organometallics* **1999**, *18*, 2700–2706.

[16] L.-C. Song, Q.-M. Hu, H.-T. Fan, B.-W. Sun, M.-Y. Tang, Y. Chen, Y. Sun, C.-X. Sun, Q.-J. Wu, *Organometallics* **2000**, *19*, 3909–3915.

[17] L.-C. Song, H.-T. Fan, Q.-M. Hu, *J. Am. Chem. Soc.* **2002**, *124*, 4566–4567.

[18] A. Winter, L. Zsolnai, G. Huttner, *J. Organomet. Chem.* **1983**, *250*, 409–428.

[19] A. Shaver, P. J. Fitzpatrick, K. Steliou, I. S. Butler, *J. Am. Chem. Soc.* **1979**, *101*, 1313–1315.

[20] D. Seyferth, R. S. Henderson, L.-C. Song, *Organometallics* **1982**, *1*, 125–133.

[21] D. Seyferth, G. B. Womack, C. M. Archer, J. P. Fackler, Jr., D. O. Marler, *Organometallics* **1989**, *8*, 443–450.

[22] H. Patin, G. Mignani, C. Mahé, J.-Y. Le Marouille, T. G. Southern, A. Benoit, D. Grandjean, *J. Organomet. Chem.* **1980**, *197*, 315–325.

[23] J.-M. Lehn, *Supramolecular Chemistry, Concepts and Perspectives*, VCH, Weinheim, **1995**.

[24] R. B. King, *Organometallic Syntheses, Vol. 1*, *Transition-Metal Compounds*, Academic Press, New York, **1965**, p. 95.

[25] C. J. Pedersen, *J. Am. Chem. Soc.*, **1967**, *89*, 7017–7036.

[26] A. J. Speziale, *Org. Synth. Collect.* **1963**, *4*, 401–403.

[27] L. Horner, P. Beck, V. G. Toscano, *Chem. Ber.* **1961**, *94*, 2122–2125.

[28] W. Ried, F.-J. Königstein, *Chem. Ber.* **1959**, *92*, 2532–2542.

[29] W. Wenner, *J. Org. Chem.* **1952**, *17*, 523–528.

[30] H. Stone, H. Schechter, *Org. Synth.* **1950**, *30*, 33–34.

[31] R. B. King, *Organometallic Syntheses, Vol. 1*, *Transition-Metal Compounds*, Academic Press, New York, **1965**, p. 175.

[32] A. Maaninen, T. Chivers, M. Parvez, J. Pietikäinen, R. S. Laitinen, *Inorg. Chem.* **1999**, *38*, 4093–4097.

Received: September 12, 2002 [F4423]

